

SIMULATION AND MULTIPLICITY OF STEADY STATES OF CSTRs FOR FREE RADICAL POLYMERIZATION WITH THE GEL EFFECT

A Thesis Submitted
in Partial Fulfilment of the Requirements
for the Degree of
MASTER OF TECHNOLOGY

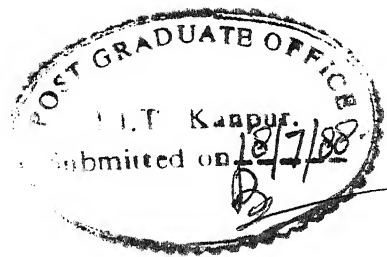
by
SADHAN CHANDRA JANA

to the
**DEPARTMENT OF CHEMICAL ENGINEERING
INDIAN INSTITUTE OF TECHNOLOGY KANPUR
JULY, 1988**

17 1988
CENTRAL LIBRARY
Acc. No. **A** 103059

Thesis
660.28448
J2518

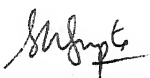
CHE-1988-M-JAN-SIM



CERTIFICATE

This is to certify that the present work
'SIMULATION AND MULTIPLICITY OF STEADY STATES OF
CSTRs FOR FREE RADICAL POLYMERIZATION WITH THE GEL
EFFECT' has been carried out by Mr. Sadhan Chandra
Jana under my supervision and this has not been
submitted elsewhere for a degree.

July, 1988


(Santosh K. Gupta)
Professor
Department of Chemical Engineering
Indian Institute of Technology
Kanpur

ACKNOWLEDGEMENTS

It is my pleasure to acknowledge my debt to Dr. Santosh Kumar Gupta. Throughout my stay with him, I have been exposed to his tremendous enthusiasm, vast knowledge and limitless inspiration. This work would have been incomplete without his untiring help and lively discussions about the intricate parts of this study. I acknowledge the amicable behaviour, I have got from my friends, Bir Kapoor, Subhasis Bhattacharya, Dipak Sarkar and Vimal Katyar, that made my sojourn at IIT Kanpur very enjoyable.

I express my sincere gratitude to Mr. J.P. Sharma, for neat and effecient typing and Mr. A.K. Ganguly for preparing drawings.

Sadhan Chandra Jana

CONTENTS

LIST OF FIGURES	iv	
LIST OF TABLES	vi	
NOMENCLATURE	vii	
ABSTRACT	xi	
CHAPTER		
I	INTRODUCTION	1
II	FORMULATION	10
III	RESULTS AND DISCUSSIONS	25
IV	CONCLUSIONS	46
V	SUGGESTIONS FOR FUTURE WORK	47
	REFERENCES	48

LIST OF FIGURES

<u>Figure</u>	<u>Title</u>	<u>Page</u>
1	Schematic diagrams of the six possible multiplicity patterns	7
2	Schematic presentation of the continuous flow stirred tank reactor (CSTR).	12
3	Comparison of batch reactor simulation results for PMMA polymerization using parameter values e_t^o , e_p^o , E_{e_t} and E_{e_p} from Table VIII (column b) with experimental data (o, ●) at 90°C	27
4	Comparison of batch reactor simulation results for PMMA polymerization using parameters e_t^o , e_p^o , E_{e_t} and E_{e_p} from Table VIII (column c and d) with experimental data (o,) at 90°C	30
5	CSTR simulation results with parameters e_t^o , e_p^o , E_{e_t} and E_{e_p} from Table VIII (column e)	33
6	CSTR simulation results using parameters, e_t^o , e_p^o , E_{e_t} and E_{e_p} from Table VIII (column a and e)	34
7	CSTR simulation results with parameters e_t^o , e_p^o , E_{e_t} and E_{e_p} from Table VIII (column e) for $e_t = e_t ([I])$ ——— for $e_t = e_t ([I]_o)$	36

8	Comparison of CSTR simulation results with parameters θ_t^o , θ_p^o , E_{θ_t} and E_{θ_p} from Table VIII (column e) with the results reporduced from Carrat et al.'s ⁴¹ plot.	37
9	Batch reactor simulation results using Ross and Laurence gel effect model. Results for varying, $f = 0.487-2.51$ (dotted line) and $f = 0.58$ are presented (solid line)	38
10	Comparison of CSTR simulation results using Ross and Laurence gel effect model with Chiu et al.'s model. Parameters θ_t^o , θ_p^o , E_{θ_t} and E_{θ_p} are taken from Table VIII (column e), $f = 0.58$	40
11	Bifurcation behaviour of CSTRs for solution polymerization of PMMA without gel effect.	42
12	CSTR simulation results for free radical solution polymerization of PMMA using different values of the parameters α and β	43
13	Bifurcation behaviour of CSTRs for solution polymerization of PMMA with gel effect.	44
14	Simulation results with gel effect for solution polymerization of PMMA in CSTRs using different values of α and β .	45

LIST OF TABLES

<u>Table</u>	<u>Title</u>	<u>Page</u>
I	Kinetics of free radical polymerization	2
II	Species balance equations for a CSTR	13
III	Species balance equations in dimensionless form	15
IV	Species balance equations for isothermal batch reactor	18
V	Constitutive gel and glass effect equations	19
VI	Values of parameters for PMMA	24
VII	θ_t and θ_p values used by Chiu et al. ¹³ in fitting experimental data of Marten-Hamielec ⁷	26
VIII	Comparison of the values of the parameters θ_t^o , θ_p^o , E_{θ_t} and E_{θ_p} used by various workers.	29

CHAPTER V

SUGGESTIONS FOR FURTHER STUDY

For the correct prediction of parameter values, for which the CSTRs exhibit five different patterns of study state multiplicity, a specific α - β plot is necessary. It can be generated by accounting for the stiffness of the functions F , F_{x_1} , F_{xx_1} and F_{Da} and simultaneous solution of the defining equations of hysteresis and isola varieties. Further, the study of stability of these multiple solutions is necessary for the efficient control of the reactor.

NOMENCLATURE

A, B	Dimensionless terms in the expression of C (Table II)
C_p	Specific heat of the reaction mixture
Da	Damkohler number
D_n	Dead polymer molecule having n repeating units
E_d	Activation energy for initiator decomposition
E_p	Activation energy of chain propagation
E_t	Activation energy of chain termination
$E_{\theta_t}, E_{\theta_p}$	Activation energies in θ_t, θ_p expressions (Table II)
f	Initiator efficiency
f_s	Solvent volume fraction in the feed
h	Heat transfer coefficient to reactor
$(-\Delta H_r)$	Heat of propagation reaction
I	Initiator
k_d	Initiator decomposition rate constant
k_d^o	Pre-exponential factor of initiator decomposition rate constant

k_p	Propagation rate constant
k_{p_o}	Propagation rate constant in absence of gel-effect
$k_{p_o}^o$	Pre-exponential factor of k_{p_o}
k_t	Termination rate constant
k_{t_c}	Combinational termination rate constant
k_{t_d}	Termination rate constant by disproportionation
k_{t_o}	Termination rate constant in absence of gel-effect
$k_{t_o}^o$	Pre-exponential factor of k_{t_o}
M	Monomer concentration
$P_n.$	Growing radical having n repeating units
Q	lit solution/min of product
Q_m	lit monomer/min in product
Q_o	lit solution/min of feed
Q_p	lit polymer/min in product
Q_s	lit solvent/min in product
Q_{m_o}	lit monomer/min in feed
Q_{p_o}	lit polymer/min in feed
Q_{s_o}	lit solvent/min in feed
R.	Primary radical

R	Universal gas constant
S	Dimensionless parameter (Table IV)
T	Reactor temperature
T_c	Coolant temperature
T_f	Feed temperature
T_m, T_p	Glass transition temperature of monomer and polymer respectively
V	Volume of the reactor
V_f	Free volume fraction
X_1	Conversion of monomer to polymer
X_2	Fractional conversion of initiator
X_3	Dimensionless temperature

Greek Letters

α	Dimensionless heat transfer parameter
β	Dimensionless heat of reaction
δ	Dimensionless coolant temperature
ϵ	Dimensionless density change of the reaction mixture, $(\frac{\rho_p - \rho_m}{\rho_p})$.
Ξ	$f_s/(1-f_s)$

ϕ_m	Volume fraction of monomer ($\frac{1-X_1}{1-\varepsilon X_1+\varepsilon}$)
ϕ_p	Volume fraction of polymer ($\frac{X_1(1-\varepsilon)}{1-\varepsilon X_1+\varepsilon}$)
ρ_m	Density of the monomer at the reactor temperature
ρ_{mo}	Density of the monomer at the feed temperature
ρ_s	Density of solvent
θ_p, θ_t	Characteristic migration times for propagation and termination respectively
θ_p^o, θ_t^o	Pre-exponential factors of θ_p, θ_t respectively
τ	Dimensionless mean residence time
λ_o	Total concentration of the live polymer
ε	$f_s/(1-f_s)$

Symbols

$[\quad]$	Concentration, mol/lit
$[\quad]_o$	feed concentration, mol/lit

Subscripts

m	Monomer
o	Inlet value

Superscripts

o	Pre-exponential value
---	-----------------------

ABSTRACT

An attempt has been made to improve the gel and glass effect correlations of Chiu et al. Soong and coworkers adopted the model of Chiu et al. and used different values of the parameters in the correlations for θ_t and θ_p . No consistent set of parameters were obtained in their studies. Improved parameter values obtained herein match the CSTR simulation results of Carrat et al. very well. Steady state multiplicity patterns of continuous flow stirred tank reactors (CSTRs) with gel effect are explored. Above an average conversion of 40%, the presence of gel effect cannot be neglected. Only hysteresis type multiplicity could be obtained using simulation results. The stiffness and sensitivity of the defining equations of hysteresis and isola varieties made it impossible to solve them numerically to give a bifurcation diagram.

CHAPTER I

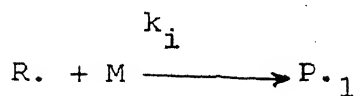
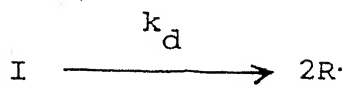
INTRODUCTION

There has been a spate of research activity in the area of modeling and control of free radical polymerization reactors over the past few years. With the improved understanding of polymerization kinetics and reactor behaviour, aided by the implementation of sophisticated reactor control algorithms, current research is directed towards the control of polymer properties. For over four decades, both free radical bulk and solution polymerizations have been a matter of study. From the vast array of experimental data with different systems (e.g., polystyrene, PS, polymethyl methacrylate, PMMA) in this field, it is well established that the classical low conversion free radical kinetics^{1,2} (See Table I for mechanism) cannot be applied over the entire course of the reaction, especially at high conversions. Even under isothermal conditions, many such polymerization systems exhibit a large autoacceleration of the rate of polymerization, associated with an increase in the molecular weight of the polymer produced. This autoacceleration, the result of a very rapid decrease in the rate constant associated with chain-termination (k_{tc} and k_{td}) due to the introduction of severe diffusional limitations, is known as the gel or Trommsdorff³ effect. With the progress of reaction beyond the gel-effect,

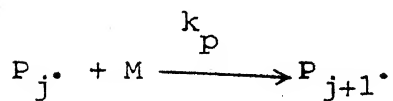
TABLE I

KINETICS OF FREE RADICAL POLYMERIZATION

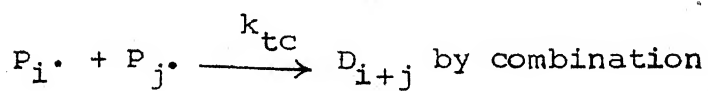
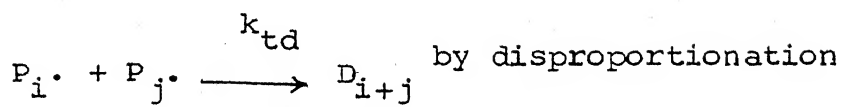
INITIATION



PROPAGATION



TERMINATION



a point may be reached where even the diffusion of the monomer to the reactive radical sites is severely curtailed. This phenomenon accounts for a drastic decrease in the propagation rate constant, k_p , and is known as the glass effect. In the past few decades, several researchers have tried to explain experimental data by improving the kinetic model to account for the gel and glass-effects. All such improvements are backed by some physical assumptions. Friis and Hamielec⁴ and Ross and Laurence⁵ used simple empirical methods to describe such polymerization kinetics. They correlated an apparent termination rate constant with various system parameters, such as conversion, temperature and free volume. A second string of workers approached the problem of gel effect by making some empirical statements about the molecular weight and conversion dependence of the termination rate constant, k_t , using either qualitative analogies or experimental results on polymer transport phenomena or both. Of these workers, the work of Cardenas and O'Driscoll⁶ (COD) and Marten and Hamielec⁷ (MH) are important. In the COD model, the polymer species are divided into two populations, one with the degree of polymerization (DP) less than a critical value and the other with a degree of polymerization greater than the critical value. The critical degree of polymerization dictates the onset of the gel effect. The population with a DP less than $(DP)_{crit}$ is assigned a termination rate constant ' k_{t_0} ' which is the value in the

absence of the gel-effect. But the termination rate constant for the population with $DP > DP_{crit}$, k_t , the apparent rate constant, is an inverse function of the number-average degree of polymerization and the polymer volume fraction. In the MH model it is assumed that k_t depends on the polymer concentration and molecular weight. Both these model are good in fitting experimental data, but are based on totally different and nonequivalent physical assumptions and use different dependences of k_t upon concentration and molecular weight. However, the above models are empirical and are not tested against other solution properties of the system over the range of conditions of the experiment. Moreover, in these models, the diffusion behaviour of the radicals has been expressed in an adhoc manner which is flexible enough so that it could be adjusted to fit experimental data. Tulig and Tirrel⁸ developed a model using classical diffusion-controlled reaction kinetics and related the termination rate constant to the diffusion constant of the growing radical. The model can fit experimental data on conversion vs. time and molecular weight vs. conversion upto about 70 or 75% conversion. Besides these, a number of researchers⁹⁻¹² in an attempt to determine the effects of concentration, viscosity and molecular weight on the rate of polymerization, have carried out kinetic experiments. But even with such extensive research, a consistent understanding of the

molecular processes controlling the rate of polymerization could not emerge. Chiu et al.¹³ recently focussed on this aspect and modeled this phenomena using a molecular view point. They developed a mathematical model to describe the gel and glass effects from a fundamental molecular phenomena. It does not need any artificially imposed break points either in the viscosity or in the molecular weight vs. concentration plots, to indicate the onset of diffusional limitations to the termination and propagation steps. Model parameters are linked to the operating variables of the process, especially to the reaction temperature. Moreover, one unified equation is sufficient to evaluate k_p and k_t for the entire course of the reaction. They have fitted the experimental data at all the three temperatures, 50°, 70° and 90°C, for which good isothermal batch data is available, using gross values of the model parameters. For these reasons , the model of Chiu et al.¹³ is followed in the present work.

In the last two decades, remarkable progress has also been made in the understanding of the complex steady-state multiplicity patterns shown by continuous flow stirred tank reactors (CSTRs). For a single, exothermic, first order reaction occuring in a CSTR, changes in the flow rate (hence, residence time) can lead to complex multiplicity of steady-states of the reactor. Zeldovich and Zysin¹⁴ were the first to indicate four different multiplicity patterns for a very

high activation energy of the reaction. Although earlier unnoticed, this work was later confirmed by Furusawa and Nishimura¹⁵, and Hlavacek et al.¹⁶. Uppal, Ray and Poore¹⁷ developed an intricate scheme to investigate the multiplicity pattern for any specific set of parameters, which was later simplified by Huang and Varma¹⁸. Golubitsky and Keyfitz¹⁹ applied singularity theory to prove that, for such systems, upto six different steady-state multiplicity patterns are possible (Figure 1). However, their analysis cannot predict the multiplicity pattern for any set of physical parameters values. Balakotaiah and Luss²⁰ developed a simple technique for the exact prediction of the multiplicity pattern for any set a parameter values. They extended their technique to find the multiplicity pattern for reactions with any rate expression²¹⁻²⁵. Although these are devoted only to single, exothermic reactions, considerable progress has been made in its application to polymerization reactors also. Indeed, in recent years, steady state characteristics and dynamic behaviour of various types of polymerization reactors have been studied extensively²⁶⁻³⁴. Hamer et al.³⁰ studied the free radical solution polymerization in CSTRs and identified multiple steady states, limit cycles and oscillatory phenomena depending upon the values of the solvent volume fraction and the heat transfer parameter. They showed that upto six different types of multiplicity patterns are possible.

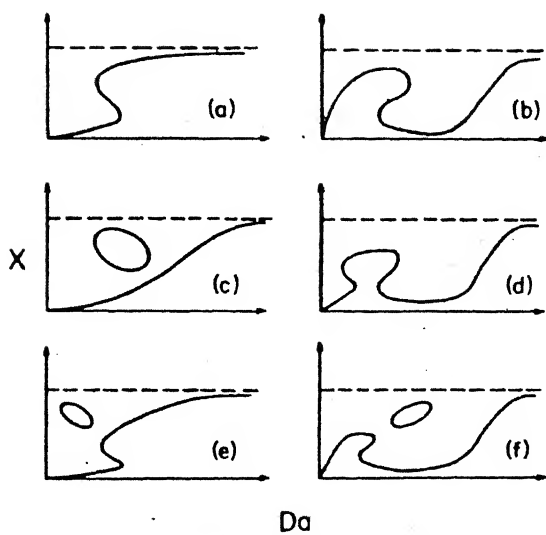


FIGURE 1 Schematic diagrams of the six possible multiplicity patterns.

Schmidt et al.³⁴ confirmed the isolated branch in the conversion vs. residence time plot (called isola) experimentally. They indicated that operating the reactor at isolas may help obtain high conversions at low residence times. They used coolant temperature, reactor heat transfer coefficient and feed solvent concentration as parameters and showed that these parameters can have an enormous effect on reactor behaviour. Jaisinghani and Ray²⁸ performed an analysis of the reactor behaviour by assuming that the initiator concentration remain unchanged for the course of the reaction i.e., initiator consumption is negligibly small. They argued that, in commercial practice, the effective initiator concentration in the reactor can be maintained nearly constant over a wide range of conversions, when the initiators are slowly decomposing and are used in high concentration in the feed. They identified the multiple steady states and unstable limit cycles. Recently, Choi³⁵ followed the technique of Balakotaiah and Luss²⁰ to investigate the multiplicity patterns of CSTRs for free radical solution polymerization. He developed the model for solution polymerization (solvent volume fraction $f_s > 0.6$) of methylmethacrylate with constant initiator concentration and no gel effect and analysed it using heat of reaction, heat transfer coefficient, coolant temperature and activation energies in the form of various dimensionless parameters. He identified five regions of parameter values which were

used to exhibit five different types of multiplicities. He then applied the same methodology to the case of variable initiator concentration i.e., when the change in the initiator concentration cannot be neglected. However, Choi's methodology does not have any provision to include the gel effect. In fact, for bulk polymerization systems or for solution polymerization systems with $f_s < 0.6$, the presence of gel effect cannot be overruled.

In the first part of the present work, an attempt has been made to improve the correlations for the gel effect. There are two parameters, θ_t and θ_p (See Table II) the model of Chiu et al.¹³ which need to be improved in order to match experimental data ^{on batch reactor}. In the second part, a study of free radical solution polymerization of methyl methacrylate in CSTRs has been carried out, with an objective of investigating the steady state multiplicity patterns of the reactor. The influence of both the gel and glass effects has been accounted for in the present work, using Chiu et al.'s gel¹³ effect model with improved θ_t and θ_p correlations obtained in the first part.

CHAPTER II

FORMULATION

The first step in formulation is to identify the kinetic mechanism. The kinetics of free radical polymerization is summarized in Table I. The reaction mechanism adopted here consists of three major steps, characteristic of all free radical polymerization processes. They are initiation, propagation and termination. In the chain initiation step, free radicals are generated by the thermal decomposition of an initiator such as AIBN (2, 2' - azo bisisobutyronitrile). They result in two primary free radicals, R^\bullet . In chain propagation, primary radicals thus generated quickly react with monomer to form long polymer radicals, P_n^\bullet : Propagation ends when either a glass is formed (and $k_p \rightarrow 0$) or an equilibrium monomer concentration is reached. Termination occurs when two radicals react via a bimolecular process. Radicals could terminate via two paths. The microradicals can combine to form a single dead polymer chain (called combination) or form two dead chains (called disproportionation). Although radical transfer to solvent and to monomer has to be accounted for for accurate prediction of molecular weights, in this study, for the sake of simplicity, these are neglected. Also neglected are the branching reactions, thermal initiation of monomer, and all other transfer reactions. These are not expected to influence multiplicity characteristics significantly.

The second step is to develop the species mass balance and energy balance equations from the kinetic scheme of Table I. A CSTR of volume V is considered here with inlet and outlet streams as in Figure 2. The symbols are explained in the Nomenclature. Details of the balance equations are presented in Table II. A little reflection on the definitions of the Q and M terms shows that the volumetric flow rate of the product stream is given by the sum of the contributions of the monomer (m), polymer (p) and solvent (s):

$$Q = Q_m + Q_p + Q_s \quad (1)$$

where

$$Q_s = \epsilon Q_{mo} \quad (a)$$

$$Q_p = \frac{M_o X_1}{\rho_p} \quad (b)$$

$$Q_m = \frac{M_o (1 - X_1)}{\rho_m} \quad (c) \quad (2)$$

In Eqn. 2 $M_o X_1$ is the gm of monomer/min, being converted into polymer, $\epsilon = f_s/(1-f_s)$, and f_s is the volume fraction of solvent in the feed. It is assumed that the density of the solvent is constant, and that the feed consists only of monomer, initiator and solvent.

The monomer conversion, X_1 is defined in Table III. Defining the volume contraction parameter, ϵ , as

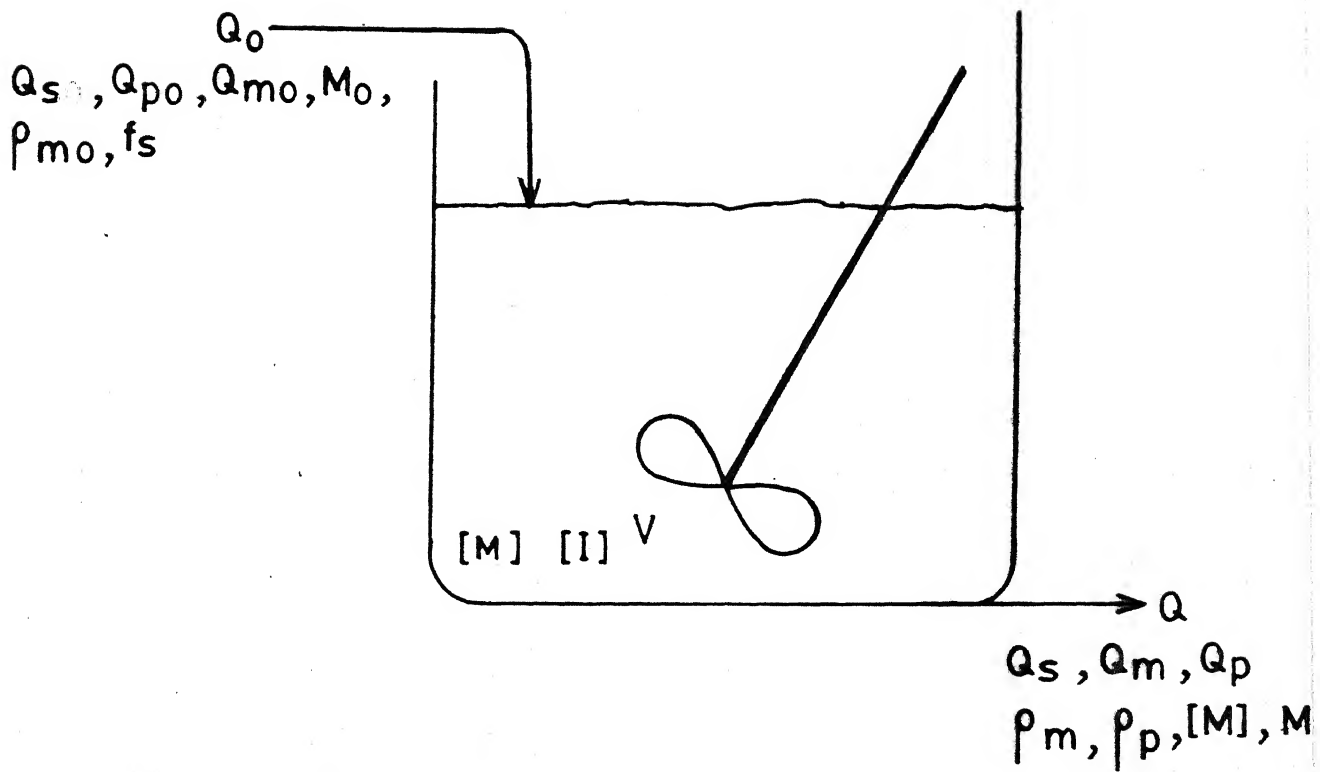


Figure 2 : Schematic presentation of the continuous flow stirred tank reactor (CSTR).

TABLE II

SPECIES BALANCE EQUATIONS FOR A CSTR [Fig.2]

Monomer Balance:

$$Q_0 [M]_0 - Q [M] = k_p \lambda_0 [M] V \quad (a)$$

Initiator Balance:

$$Q_0 [I]_0 - Q [I] = k_d [I] V \quad (b)$$

Live Radical Balance:

$$n = 1 :$$

$$Q [P_1] = (2f k_d [I] - k_t [P_1] \lambda_0 - k_p [P_1][M]) V \quad (c)$$

$$n \geq 2 :$$

$$Q [P_n] = (k_p [M] ([P_{n-1}] - [P_n]) - k_t [P_n] \lambda_0) V \quad (d)$$

Energy Balance:

$$Q_0 \rho_{mo} C_P (T_f - T) + (-\Delta H_r) k_p [M] \lambda_0 V - hA (T - T_c) = 0 \quad (e)$$

$$\varepsilon = \frac{\rho_p - \rho_m}{\rho_m} \quad (3)$$

and with the help of Eqns. (2) and (3) Eqn. (1) can be simplified as,

$$Q = \frac{Q_o}{(1+\varepsilon)} \left[\frac{(1-\varepsilon X_1) \rho_{mo}}{\rho_m} + \varepsilon \right] \quad (4)$$

The various model equations of Table II can be made dimensionless with the help of Eqn. (4). They are presented in Table III. The various dimensionless variables and parameters are also defined there.

For the live radical balance, the quasi-steady state approximation (QSSA) can be taken for the live polymer. Although QSSA for live polymer fails at high conversion for nonisothermal batch reactors, several researchers have used the same for free radical solution polymerization in CSTRs^{31,33}, without much error. Thus equation (d) of Table III reduces to

$$\lambda_o^2 = \frac{2f k_d [I]_o (1 - X_2)}{s k_t} \quad (5)$$

Equations (a), (b) of Table III and Eqn. (5) can be combined into a single equation,

$$F(X_1, Da, \alpha, \beta, \delta) = \frac{2f [I]_o Da^2 k_p^2 k_d}{k(T_f)^2 k_t} - \frac{s^2 X_1^2}{(1 - X_1)^2}.$$

$$\left[s + \frac{k_d}{k(T_f)} Da \right] = 0 \quad (6)$$

TABLE III

SPECIES BALANCE EQUATIONS IN DIMENSIONLESS FORM

Monomer Balance:

$$-X_1 + \frac{k_p \lambda_o}{k(T_f)} \frac{(1-X_1) Da}{S} = 0 \quad (a)$$

Initiator Balance:

$$-X_2 + \frac{k_d \cdot Da}{k(T_f)} \frac{(1-X_2)}{S} = 0 \quad (b)$$

Energy Balance:

$$-X_3 + Da \frac{(1-X_1)}{S} \cdot \frac{k_p \lambda_o}{k(T_f)} - Da (X_3 - \delta) = 0 \quad (c)$$

Live Radical Balance:

$$k_t \lambda_o^2 = \frac{2f k_d [I]_o (1-X_2)}{S} - \left[\frac{(1-\epsilon X_1) \rho_{mo}}{\rho_m} + \epsilon \right]$$

$$\frac{\lambda_o}{(1+\epsilon) Da} \quad (d)$$

TABLE III (CONTD.)

where

$$x_1 = \frac{Q_o [M]_o - Q [M]}{Q_o [M]_o} = \frac{M_o - M}{M_o}$$

$$x_2 = \frac{Q_o [I]_o - Q [I]}{Q_o [I]_o}$$

$$x_3 = \frac{T - T_f}{T_f}$$

$$\alpha = \frac{h A}{\rho_{mo} C_P k(T_f) V} \quad \beta = \frac{(-\Delta H_r) [M]_o}{\rho_{mo} C_P T_f}$$

$$\delta = \frac{T_c - T_f}{T_f} \quad \tau = \frac{V}{Q_o}$$

$$E = E_p + (E_d - E_t)/2$$

$$k(T_f) = k_{p_o}^o \exp(-E/RT_f) \left(\frac{2f k_d^o [I]_o}{k_{t_o}^o} \right)^{1/2}$$

$$S = \left[\frac{(1 - x_1) \rho_{mo}}{\rho_m} + \Xi \right] / (1 + \Xi)$$

$$\Xi = f_s / (1 - f_s)$$

In order to obtain the relation between X_3 and X_1 in Table III, equation (a) is multiplied by β and then subtracted from equation (c), giving,

$$X_3 = \frac{\beta X_1}{1 + \alpha Da} + \frac{\alpha Da}{1 + \alpha Da} \quad (7)$$

For isothermal batch reactor simulation, mass balance equations relevant to the kinetic scheme of Table I, are presented in Table IV, using the present set of variables.

The constitutive equations for the gel and glass effect models of Chiu et al.¹³ and Ross and Laurence⁵ are shown in Table V. While the Ross and Laurence⁵ model shows a discontinuity in the value of k_t and k_p at the onset of the gel and glass effects respectively, the model of Chiu et al.¹³ gives k_t and k_p in the form of continuous functions, and hence these are easy to handle. Termination and propagation rate constants in the absence of the gel and glass effects predictably bear exponential relations to the reactor temperature, T . θ_t and θ_p also vary exponentially with temperature. Although θ_p does not vary with $[I]_0$, θ_t is indeed a function of $[I]_0$ ¹³ (discussed later). These functional relationships are also presented in Table V.

Eqn. (6) defines a surface in the parameter space defined as

$$\underline{p}^* = (\alpha, \beta, A, B, \delta) \quad (8)$$

TABLE IV

SPECIES BALANCE EQUATIONS FOR ISOTHERMAL BATCH REACTOR

Monomer Balance:

$$\frac{dx_1}{dt} = k_p (1-x_1) \lambda_o \quad (a)$$

Initiator Balance:

$$\frac{d[I]}{dt} = -k_d [I] + \frac{\epsilon[I]}{1-\epsilon x_1} \lambda_o (1-x_1) k_p \quad (b)$$

Live Radical Balance:

$$\frac{d\lambda_o}{dt} = \frac{\epsilon \lambda_o^2}{1-\epsilon x_1} (1-x_1) k_p + 2f k_d [I] - k_t \lambda_o^2 \quad (c)$$

TABLE V

CONSTITUTIVE GEL AND GLASS EFFECT EQUATIONS

Ross and Laurence Model⁵:

Gel Effect:

$$\frac{k_t}{k_{to}} = 0.10575 \exp [17.15 V_f - .01715 (T - 273.2)] \text{ for } V_f > 0.152$$

$$= 0.23 \times 10^{-5} \exp (75 V_f) \text{ for } V_f \leq 0.152$$

Glass Effect:

$$\frac{k_p}{k_{po}} = 1.0 \text{ for } V_f \geq 0.05$$

$$= 0.71 \times 10^{-4} \exp [171.53 V_f]$$

$$\text{where } V_f = 0.025 + \alpha_m (T - T_m) + [\alpha_p (T - T_p) - \alpha_m (T - T_m)] \phi_p$$

Model of Chiu et al.¹³:

Gel Effect:

$$\frac{k_t}{k_{to}} = \frac{1}{\frac{1 + \theta_t k_{to} \lambda_o}{C}}$$

Glass Effect:

$$\frac{k_p}{k_{po}} = \frac{1}{\frac{1 + \theta_p k_{po} \lambda_o}{C}}$$

TABLE V (CONTINUED)

where,

$$C = \exp \left[\frac{2.303 \phi_m}{A+B \phi_m} \right]$$

$$\theta_p = \theta_p^o \exp \left(-\frac{E_{\theta p}}{RT} \right)$$

$$\theta_t = \theta_t^o \exp \left(-\frac{E_{\theta t}}{RT} \right)$$

$$k_{p_o} = k_{p_o}^o \exp (-E_p/RT)$$

$$k_{t_o} = k_{t_o}^o \exp (-E_t/RT)$$

$$k_d = k_d^o \exp (-E_d/RT)$$

$$\phi_m = \frac{1-X_1}{1-X_1+\epsilon}$$

$$\phi_p = \frac{X_1(1-\epsilon)}{1-\epsilon X_1 + \epsilon}$$

and this surface is called the steady state manifold of the system. A bifurcation parameter is said to be the one which can give rise to transitions from unique to multiple solutions or vice versa in a plot of conversion vs. this parameter, for a given set of values of the other parameters. For example, dimensionless mean residence time, Da is used as a bifurcation parameter in Figure 1. Plot (e) of Figure 1 exhibits four bifurcation points (transition point between uniqueness and multiplicity) in the transition scheme of 1-3-1-3-1 solutions. According to Golubitsky and Keyfitz¹⁹, the surface in the parameter space, \underline{p}^* at which the continuous change of a parameter causes the appearance or disappearance of an S or inverse S pattern (Figure 1(a) and (b) respectively) is called the "hysteresis" variety. The following conditions are to be satisfied by the hysteresis variety²⁰:

$$F (X_1, Da, \underline{p}^*) = 0 \quad (a)$$

$$\frac{\delta F}{\delta X_1} (X_1, Da, \underline{p}^*) = 0 \quad (b)$$

$$\frac{\delta^2 F}{\delta X_1^2} (X_1, Da, \underline{p}^*) = 0 \quad (c) \quad (9)$$

Similarly, the isola variety defines a surface in the parameter space, \underline{p}^* , where the continuous change of one of the parameters causes the appearance or disappearance of an isolated branch in the conversion vs. mean residence time plot, and satisfies

Eqns. (9a), (9b) and

$$\frac{\delta F}{\delta Da} (X_1, Da, p^*) = 0 \quad (10)$$

Introduction of the influence of the gel effect on the propagation and termination rate constants makes the mass and energy balance equations very complex and consequently eqn. 6. For this reason, it is extremely difficult to eliminate Da from eqns. (9a) - (9c) to get an explicit relation between α and β for the generation of an $\alpha - \beta$ plot. Function F , in eqn. (6) is differentiated twice with respect to X_1 to give three non-linear algebraic equations in X_1, α, β, Da and δ , which can be solved simultaneously with the NAG subroutine CO5NBF to give values of X_1, α and β Da for given values of β and δ . This gives the $\alpha - \beta$ plot for the hysteresis variety. Similarly, for the isola variety, function F is differentiated once with respect to Da and the resulting equation is solved simultaneously with eqns. (9a) and (9b) to give an $\alpha - \beta$ plot for the isola variety for a given value of δ . The whole $\alpha - \beta$ plot thus generated is shown to be divided into various regions, each representing different multiplicity patterns of the conversion versus time plot. Particularly, the whole $\alpha - \beta$ plot has been divided into five major domains. Each type of multiplicity pattern can be verified by picking up parameter values from that region and generating the conversion vs. Da plot. For batch

reactor simulation and for the study of steady state multiplicity of CSTRs, PMMA polymerization in CSTRs is taken as an example and the various physical properties and parameter values for this system are presented in Table VI.

TABLE VIVALUES OF PARAMETERS FOR PMMA^{14, 31, 32}

f	=	0.58 (AIBN)
A	=	$0.168 - 8.17 \times 10^{-6} (T-387)^2$ (Ref.13)
B	=	0.03 (Ref.13)
C _p	=	0.4 cal/g °C
ρ_m	=	$0.973 - 0.001164 (T-273)$ g/cm ³ (Ref.13)
ρ_p	=	1.2 g/cm ³ (Ref.13)
E _d	=	30.66 kcal/mol (Ref.13)
E _p	=	4.35 kcal/mol (Ref.13)
E _t	=	0.701 kcal/mol (Ref.13)
E _{ep}	=	27.82 kcal/mol
E _{et}	=	34.176 kcal/mol
(-ΔH _r)	=	13.5 kcal/mol (Ref.35)
k _d ^o	=	6.32×10^{16} min ⁻¹ (Ref.13)
k _{p_o} ^o	=	2.95×10^7 lit/mol-min
k _{to} ^o	=	5.88×10^9 lit/mol-min
e _p ^o	=	5.48×10^{-16} min
e _t ^o	=	3.372×10^{-22} mol-min/lit
ε	=	$\frac{\rho_p - \rho_m}{\rho_p} = 0.1946 + 0.916 \times 10^{-3} (T-273)$ (Ref.13)
α _p	=	0.00048 (Ref.5)
α _m	=	0.001 (Ref.5)
T _p	=	387.0 (Ref.5)
T _m	=	167.0 (Ref.5)

CHAPTER III

RESULTS AND DISCUSSION

It has been mentioned earlier, that we have used the gel effect models of Chiu et al.¹³ and Ross and Laurence⁵, in our work. Results using the correlation of Chiu et al.¹³ are presented first. A careful survey of the various publications of Soong and coworkers^{13,36-39,41} reveals that they have used different values for the parameters θ_t^o , θ_p^o , E_{θ_t} and E_{θ_p} in their correlations for θ_t and θ_p (Table V). Chiu et al.¹³ had matched experimental conversion - time data on batch reactors of Marten and Hamielec⁷ at three temperatures, 50°C, 70°C and 90°C quite well, using values of θ_p and θ_t shown in Table VII. The agreement at one temperature, namely at 90°C for two different values of $[I]_o$ is shown in Figure 3 (curves a) Chiu et al.¹³ tried to correlate the three sets of values of θ_p and θ_t given in Table VII with the exponential relationships:

$$\theta_p = \theta_p^o \exp (E_{\theta_p} / RT) \quad (a)$$

$$\theta_t = \frac{\theta_t^o}{[I]_o} \exp (E_{\theta_t} / RT) \quad (b) \quad (11)$$

TABLE VII

θ_t and θ_p Values Used by Chiu et al.¹³ in Fitting
Experimental Data of Marten-Hamielec⁷.

Initiator loading, [I] ₀ mol/l	Polymerization Temperature, t°C	θ_t , min	θ_p , min
0.0258	50	1500.00	3500.00
	70	49.00	250.00
	90	3.80	30.00
0.01548	50	2330.00	3500.00
	70	83.00	250.00
	90	6.30	30.00

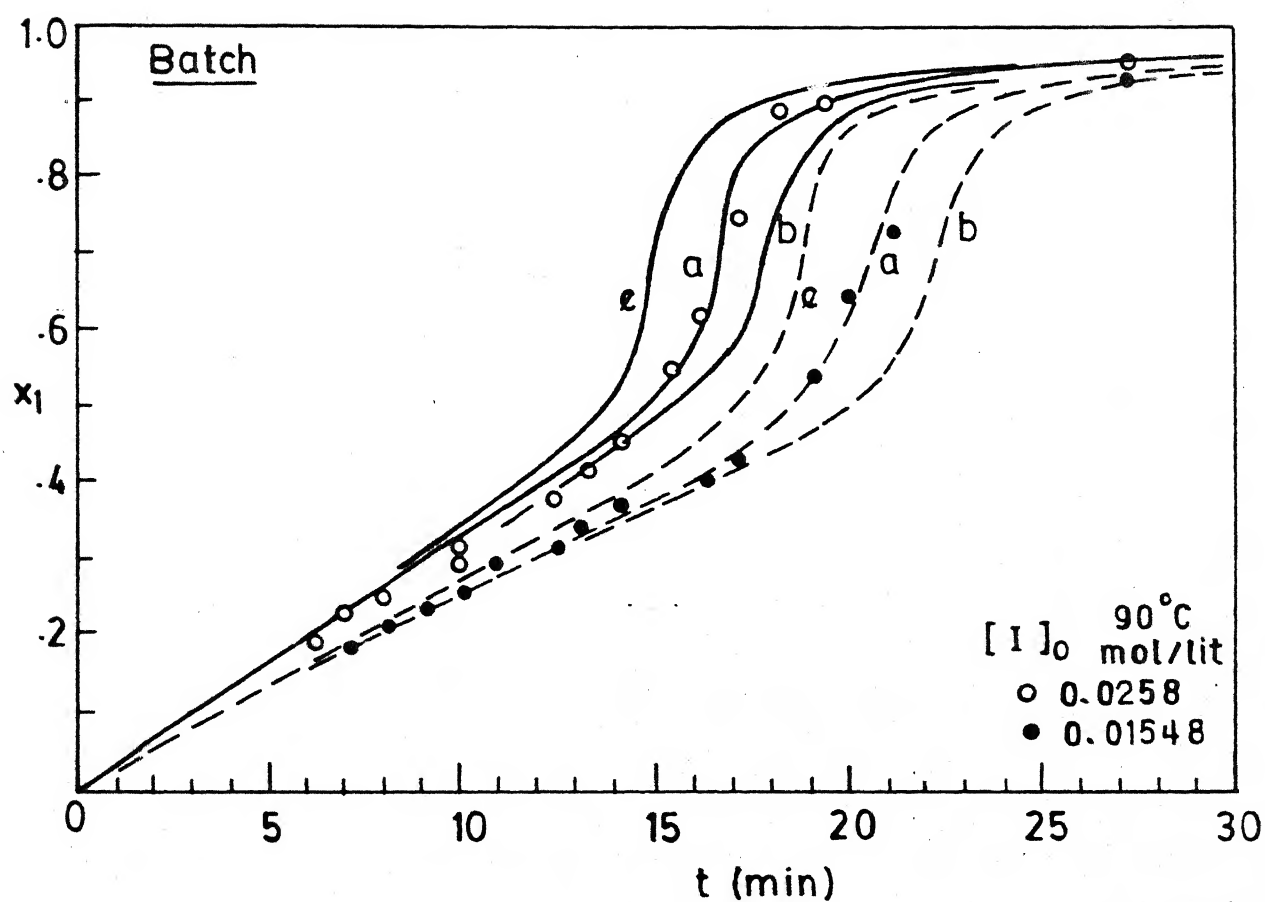


Figure 3 : Comparison of batch reactor simulation results for PMMA polymerization using parameter values θ_t^o , θ_p^o , E_{θ_t} and E_{θ_p} from Table VIII (column B) with experimental data(o,●) at 90°C

Thus, plots of $\ln (1/\theta)$ vs. $1/T$ would be straight lines, which would give the values of the parameters θ_t^o , θ_p^o , E_{θ_t} and E_{θ_p} . Their values are reported in Table VIII in column (b)⁴¹. When these values of the parameters are used at 50°C, 70°C and 90°C, it is observed that the calculated values of θ_t and θ_p are quite different from those given in Table VII. A comparison at 90°C is also shown in Table VIII. Obviously, conversion - time plots do not match experimental isothermal batch reactor data at different temperatures, as shown in Figure 3 (curves b) for 90°C. Louie et al.³⁷ used values of the four parameters θ_t^o , θ_p^o , E_{θ_t} , and E_{θ_p} as given in column d, Table VIII. Using these values it is observed from Figure 4 (curves d) that the conversion vs. time plots at constant temperature again do not match experimental results too well. Another set of parameter values were obtained by Kapur et al.⁴⁰ (Column c, Table VIII) to match nonisothermal plug-flow reactor simulation results of Baillagou and Soong^{36,38}. The corresponding results for isothermal batch reactor polymerization at 90°C are shown as curve c in Figure 4. Poor agreement with experimental results is once again observed. In the present work, we have used the values shown in column e, Table VIII, since these match constant temperature simulation results of Carrat et al.⁴¹ on CSTRs. The values shown in column b, Table VIII fail to duplicate the results in Ref. 41.

TABLE VIII

Comparison of the Values of the Parameters θ_t^o , θ_p^o , E_{θ_t} and E_{θ_p}
 Used by Various Workers^{13,36-39,41}

Curves	a	b	c	d	e
Parameters					
θ_p^o	-	5.48×10^{-16}	5.4814×10^{-16}	5.4814×10^{-16}	5.48×10^{-16}
θ_t^o	-	1.14×10^{-22}	1.1553×10^{-22}	1.1353×10^{-22}	3.372×10^{-22}
E_{θ_t} / R	-	17400	17200	17420	17200
E_{θ_p} / R	-	14000	14100	13982	14000
θ_t (at 90°C, [I] _o = 0.0258 mol/l)	3.80	2.9021	1.695	3.0538	4.9478
θ_t (at 90°C, [I] _o = 0.01548 mol/l)	6.30	4.836	2.8253	5.09	8.2462
θ_p (90°C)	30.00	30.79142	40.567	29.31	30.7914
Ref No.	13	41	40	37	Present work

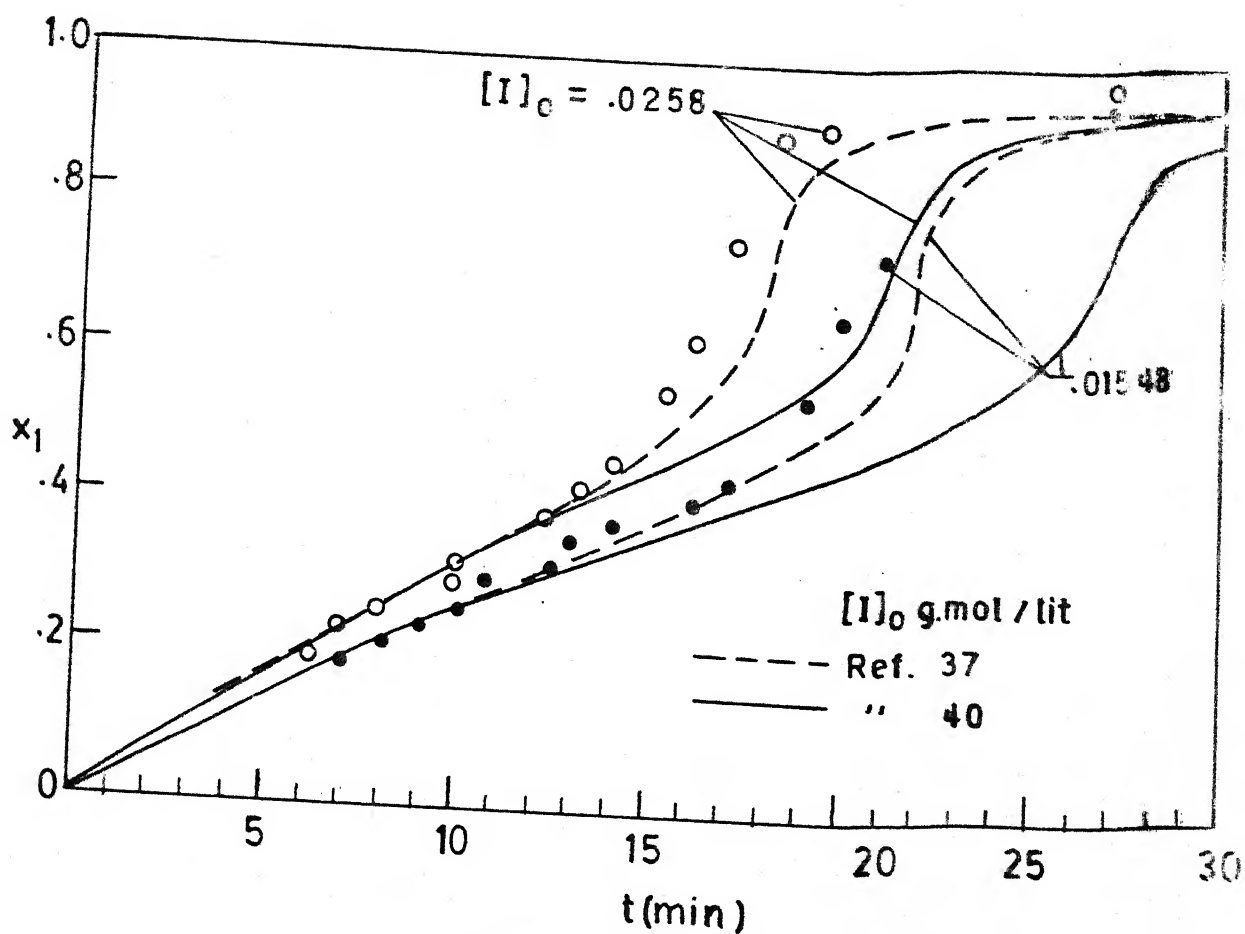


Figure 4 : Comparison of batch reactor simulation results for PMMA polymerization using parameters e_t^o , e_p^o , E_{e_t} and E_{e_p} from Table VIII (column c and d) with experimental data (o, ●) at 90°C

Figure 3 (curves e) shows that this choice of parameters again leads to poor agreement with isothermal batch reactor data.

CSTR simulation results have been generated using the parameter values of column e, Table VIII, at constant temperatures of 50°C, 60°C, 70°C, 80°C and 90°C. These are shown in Figure 5. Also shown in this figure are the simulation results of Carrat et al.⁴¹ using, the parameter values in column b, Table VIII. There is some difference observed between the two sets of results, particularly at low temperatures, but this was the best agreement we could obtain without using an elaborate optimization algorithm for obtaining the parameters. These parameters (Column e, Table VIII) have been used finally to study multiplicity of steady state in CSTRs.

Figure 6 shows some constant temperature simulation results on CSTRs using the parameters in columns a and e in Table VIII. Considerable disagreement exists, particularly at the lower temperatures between these results. It is known that θ_t is a function of the molecular weight. This, in turn, is a function of the initiator concentration in the reactor. Chiu et al.¹³, used θ_t as a function of $[I]_0$, the initiator concentration in the feed (to the batch reactor). However, we replaced this by $\theta_t = \theta_t([I])$, and accordingly,

generated simulation results on CSTRs. These are shown in Figure 7. We observed that this does not lead to very different results compared to when $[I]_0$ was used, and so to use the latter for multiplicity studies.

In summary, we observe that there is quite a confusion regarding the parameter values for θ_p and θ_t in the literature, and even the same group of workers have used different parameter values in different publications. Our own set e (Table VIII) was thus used for multiplicity studies since this gave simulation results on constant temperature CSTRs, matching those of Carrat et al.⁴¹.

Along with Chiu et al.'s¹³ model, the model of Ross and Laurence⁵ for the gel and glass effects is studied extensively to predict its applicability for free radical polymerization in batch reactors

and CSTRs. For PMMA polymerization, values of the various parameters in the model of Ross and Laurence are shown in Table IV and the model is presented in Table V. The Model of Ross and Laurence⁵ for $k_t/k_{t,0}$ and $k_p/k_{p,0}$ is used along with the $k_{t,0}$, $k_{p,0}$ values of Chiu et al.¹³ to generate batch reactor simulation results. These are shown in Figure 9. Results for varying initiator efficiency, f , as well as a constant f of 0.58 are shown. The results using variable f are close to the experimental data.

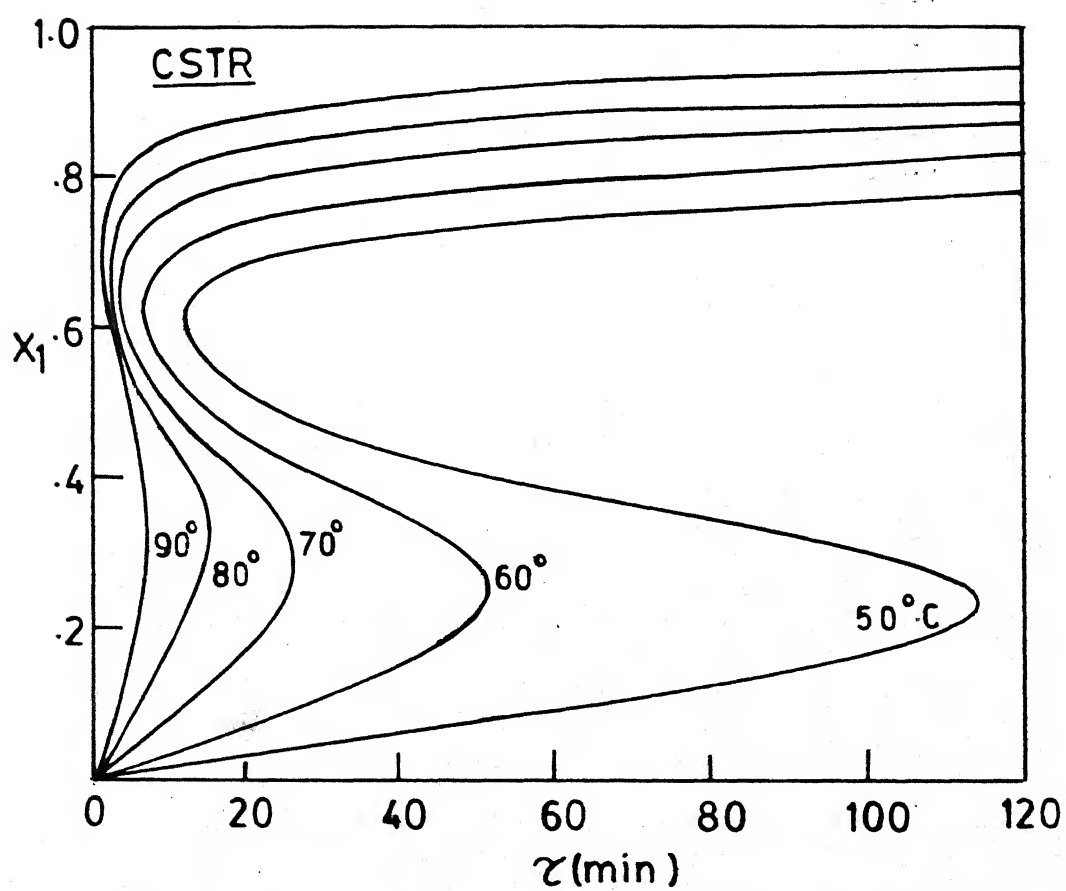


Figure 5 : CSTR simulation results with parameters θ_t^o , θ_p^o , E_{e_t} and E_{e_p} from Table VIII (column e)

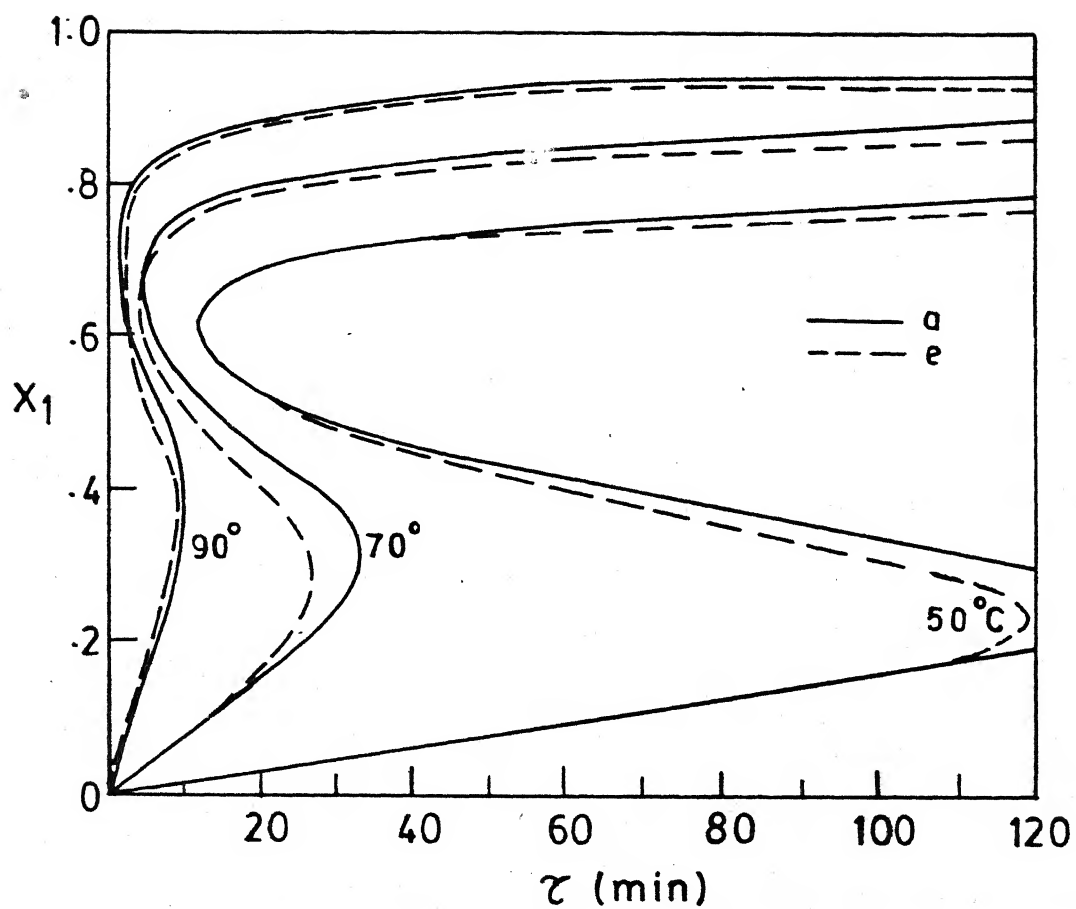


Figure 6 : CSTR simulation results using parameters, θ_t^o , θ_p^o , E_{et} and E_{ep} from Table VIII (column a and e)

CSTR simulation results are generated for constant f , using the Ross and Laurence equations for the gel and glass effects. These are plotted in Figure 10. The Ross and Laurence⁵ plots show two discontinuities in each of the curves, one at the onset of the gel effect and the other at the onset of the glass effect. These are associated with the use of different equations for the gel and glass effects in Table V before and after a critical value of the free volume. The results using the parameter values of Table VIII (column e) at 50°C, 70°C and 90°C are also shown in Figure 10 for comparison. Although they match well at 90°C, for other temperatures they do not match. Obviously multiplicity features are expected to differ significantly for the two models. In this work, we have used the Chiu et al.¹³ model for the gel and glass effects with parameter values as in column e of Table VIII to study multiplicity of steady states in CSTRs.

Choi³⁵ studied the steady state multiplicity patterns of CSTRs without the gel effect, considering free radical solution polymerization of PMMA with $f_s > 0.6$, and generated an α - β plot to depict the regions of various multiplicity patterns following the technique of Balakotaiah and Luss²⁰. However, he did not consider, in his methodology, the change in initiator concentration due to reaction, i.e., $[I] = [I]_0$. In the present study, the change in the initiator concentration

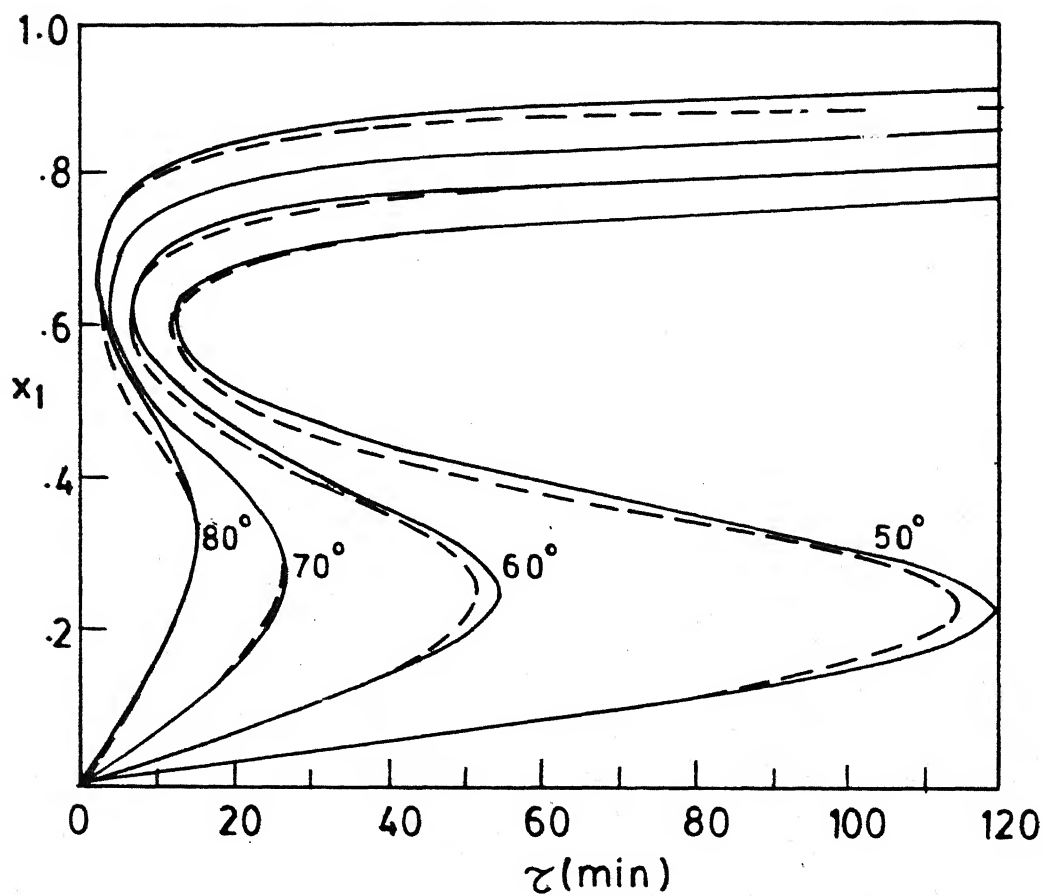


Figure 7 : CSTR simulation results with parameters e_t^o , e_p^o , E_{e_t} and E_{e_p} from Table VIII (column e)

..... for $e_t = e_t ([I])$

— for $e_t = e_t ([1]_o)$

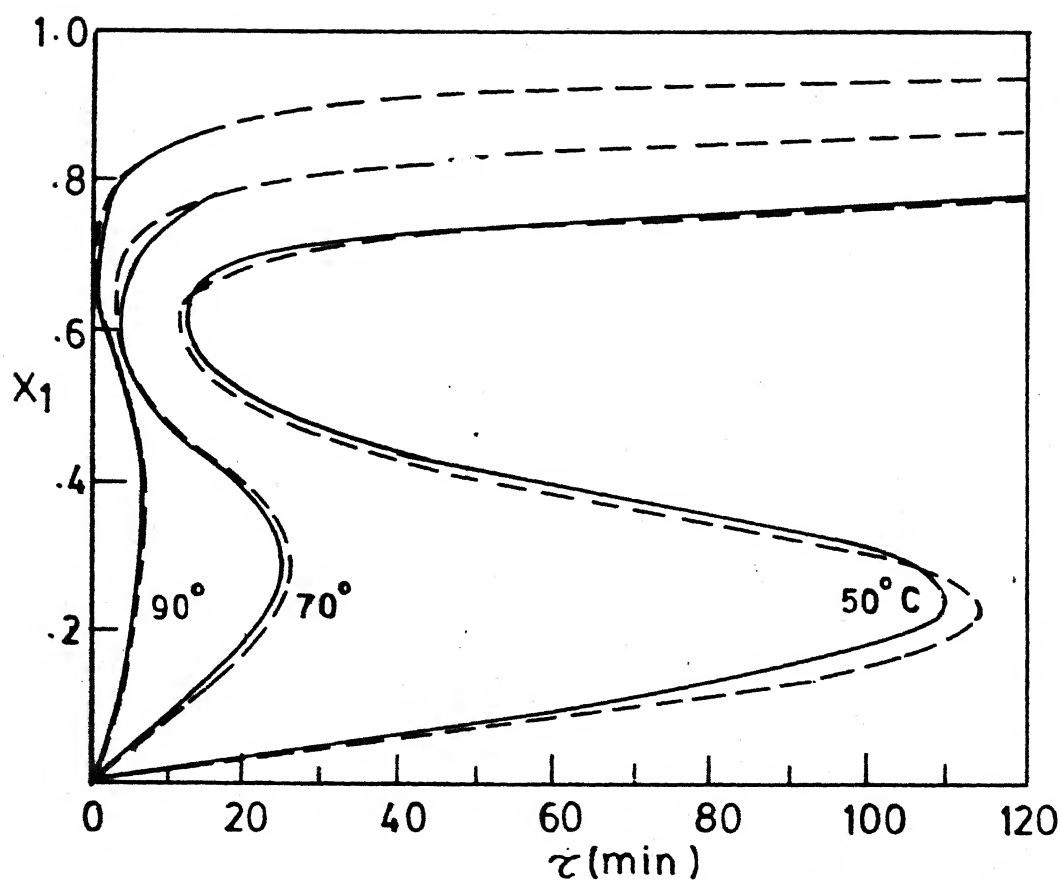


Figure 8 : Comparison of CSTR simulation results with parameters θ_t^o , θ_p^o , E_{θ_t} and E_{θ_p} from Table VIII (column e) with the results reproduced from Carrat et al.'s⁴¹ plot.

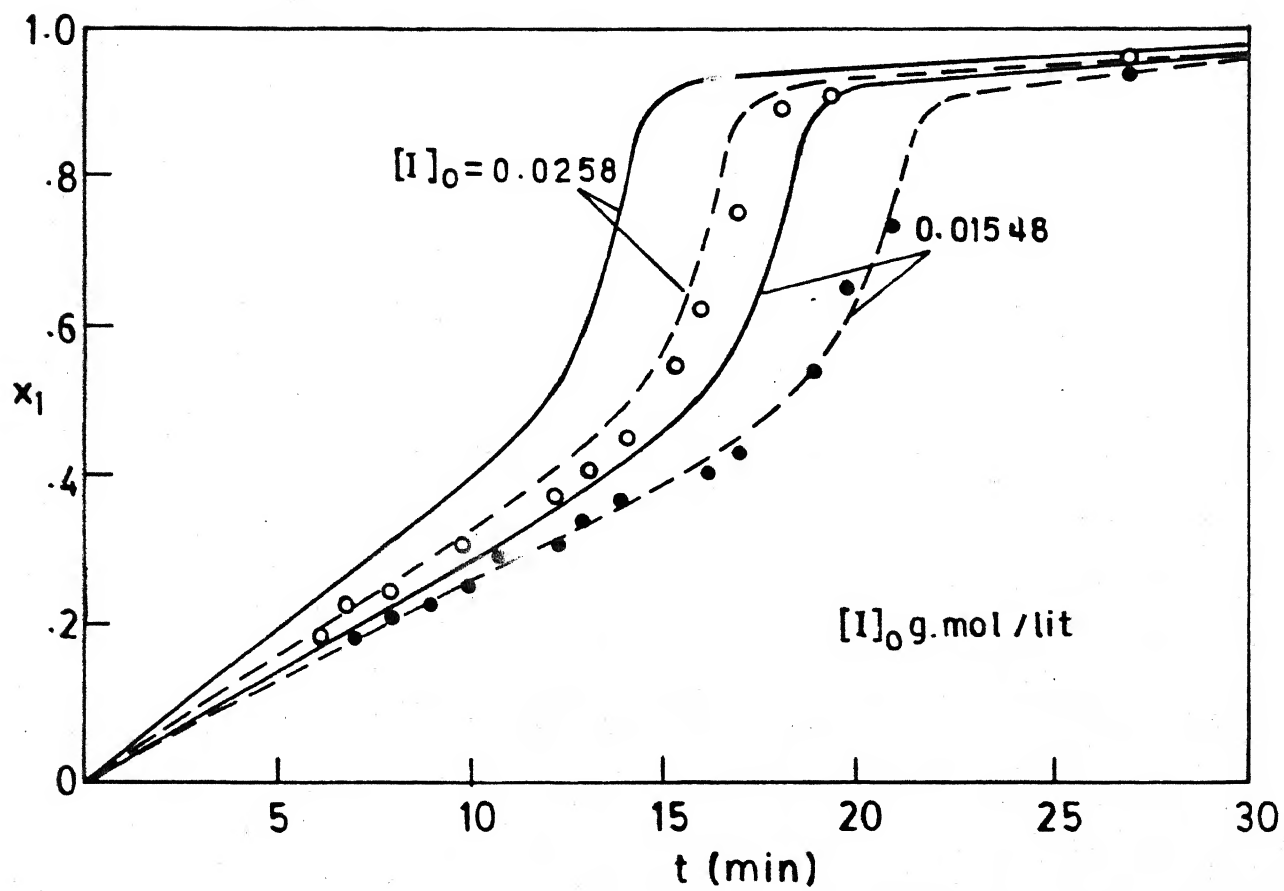


Figure 9 : Batch reactor simulation results using Ross and Laurence gel effect model. Results for varying, $f = 0.487-2.51$ (dotted line) and $f = 0.58$ are presented (solid line)

has been taken into account. Figure 11 shows the α - β plot for the hysteresis and isola varieties. In this figure, curve a shows the results of Choi³⁵ for the hysteresis variety in the absence of the gel effect. The rate constants are different than those given in Table VI. and are:

$$\begin{aligned} k_d &= 3.57 \times 10^{15} e^{-29600/RT} \text{ min}^{-1} \\ k_{po} &= 4.2 \times 10^8 e^{-6300/RT} \text{ lit}/(\text{mol-min}) \\ k_{t,o} &= 2.112 \times 10^{11} e^{-2800/RT} \text{ lit}/(\text{mol-min}) \end{aligned} \quad (11)$$

Curve b shows the hysteresis variety using the rate constants (in absence of the gel effect) of Chiu et al.¹³, as given in Table VI. In addition, the assumption $[I] = [I]_0$ is not used, nor are density changes accounted for. Similarly curves c and d give the corresponding isola variety plots for the same situations.

Simulation results for CSTRs for some values of α and β in different regions of Figure 11 are shown (Fig.12) using the rate constants (in absence of gel effect) of Table VI and not using $[I] = [I]_0$. Uniqueness, hysteresis as well as isolas are observed under appropriate conditions.

The last part of the present work is devoted to the study of steady state multiplicity with the gel and glass effects for PMMA polymerization. The functions F ,

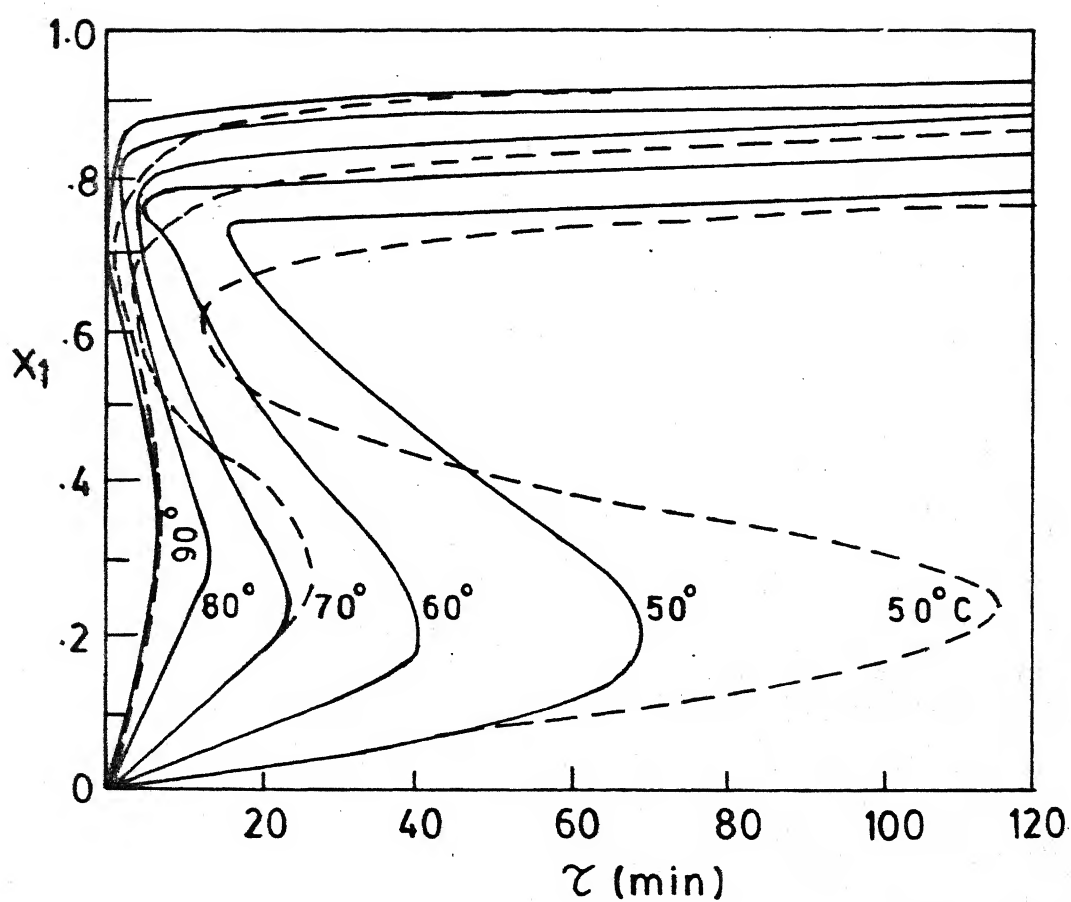


Figure 10 : Comparison of CSTR simulation results using Ross and Laurence gel effect model with Chiu et al.'s model. Parameters e_t^o , e_p^o , E_{e_t} and E_{e_p} are taken from Table VIII (column e), $f = 0.58$

F_{X_1} , $F_{X_1X_1}$ and F_{Da} are so stiff that simultaneous solution of the two sets of eqns. (9a)-(9c) and (9a), (9b) and 10 is very difficult. These simultaneous equations are very sensitive to changes in the initial guesses using the NAG subroutine C05NBF. For this reason and for lack of time, an attempt has been made to obtain an approximate $\alpha - \beta$ plot from simulation results, rather than from the technique of Balakotaiah and Luss.²⁰ These results are shown in Figure 13. Simulation results taking some of the parameter values from Figure 13 are presented in Figure 14. These plots have been generated using data in Table VI and column e of Table VIII. It is hoped that precise boundaries in the $\alpha - \beta$ plot in the presence of the gel effect will be obtained in the near future.

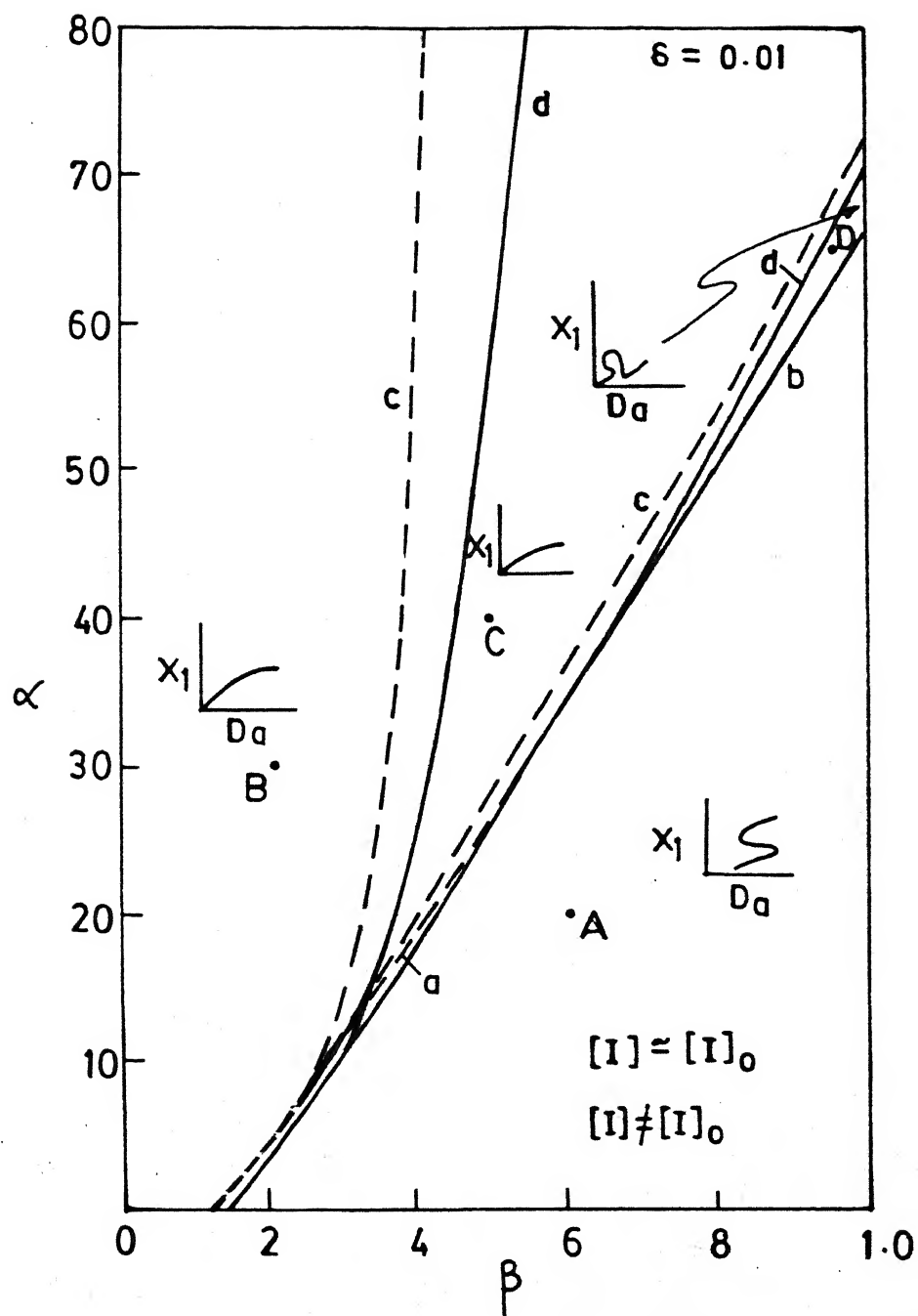


Figure 11 : Bifurcation behaviour of CSTRs for solution polymerization of PMMA without gel effect.

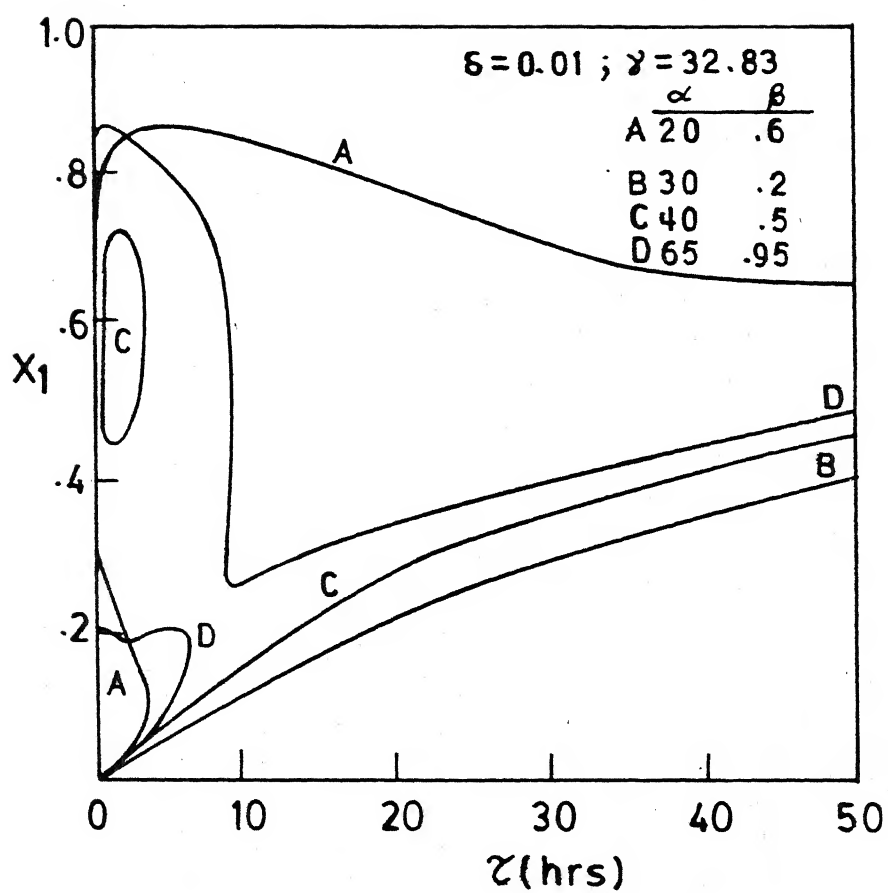


Figure 12 : CSTR simulation results for free radical solution polymerization of PMMA using different values of the parameters α and β

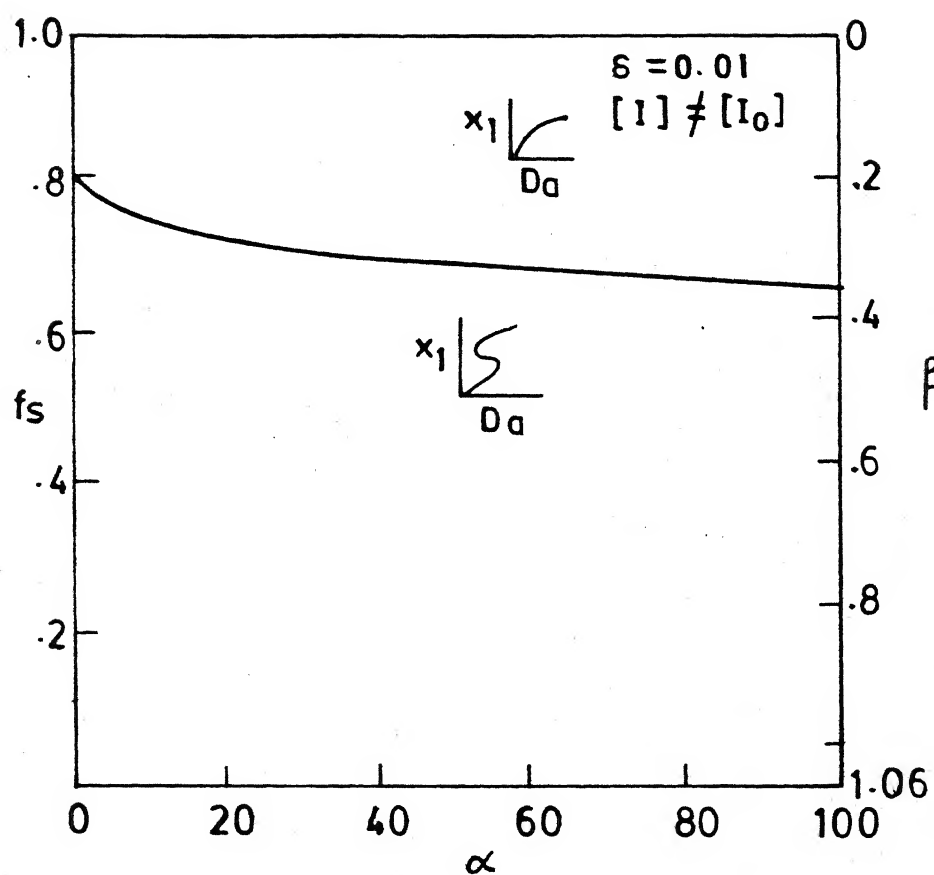


Figure 13 : Bifurcation behaviour of CSTRs for solution polymerization of PMMA with gel effect.

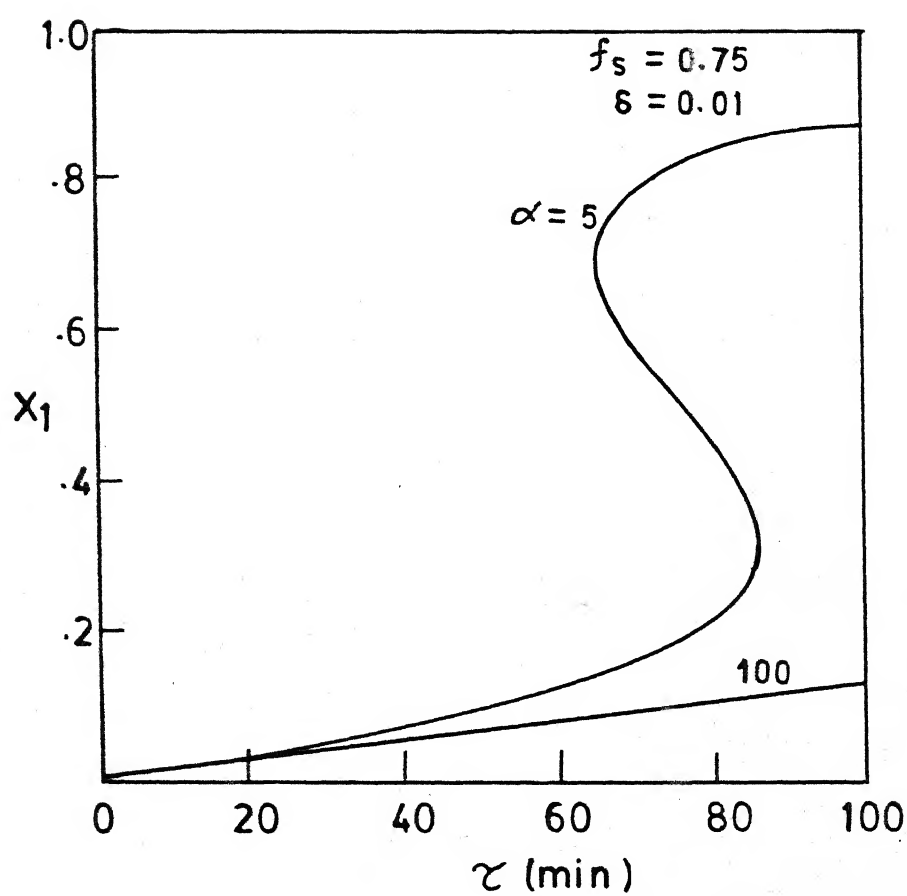


Figure 14 : Simulation results with gel effect for solution polymerization of PMMA in CSTRs using different values of α and β .

CONCLUSION

Modified parameter values for the gel effect equations of Chiu et al. give closest match to the CSTR simulation results of Carrat et al. and can be used for the study of steady state multiplicity of CSTRs with gel effect. Although only two types of steady state patterns are obtained from the simulation results for the case with gel effect a specific bifurcation diagram is needed for the possibility of other types of steady state patterns in this case. A knowledge of stability of these multiple solutions may help efficient control of the reactor.

REFERENCES

1. P.J. Flory, Principles of Polymer Chemistry, Cornell University Press, Ithaca, NY, 1953.
2. F.W. Billmeyer, Textbook of Polymer Science, Wiley - Interscience, New York, 1964.
3. E. Trommsdorff, H. Kohle, P. Lagally, Macromol. Chem., 1, 169 (1948).
4. N. Friis and A.E. Hamielec, Polym. Prepr. Am. Chem. Soc., Div. Polym. Chem., 16, 192 (1975).
5. R.T. Ross and R.L. Laurence, A.I.Ch.E. Symp. Ser., 160, 74 (1976).
6. J. Cardenas and K.F. O'Driscoll, J. Polym. Sci., Polym. Chem. Ed., 14, 883 (1976).
7. F.N. Marten and A.E. Hamielec, ACS Symp. Ser., 104, 43 (1979).
8. T.J. Tulig and M. Tirrell, Macromolecules, 14, 1501 (1981).
9. S.W. Benson and A.M. North, J. Am. Chem. Soc., 81, 1339 (1959).
10. A.M. North and G.A. Reed, Trans. Faraday Soc., 57, 859 (1961).
11. B.W. Brooks, Proc. R. Soc. London, Ser. A, 357, 183 (1977).

12. K.A. High, H.B. Lee and D.T. Turner, Macromolecules,
12, 332 (1979).
13. W.Y. Chiu, G.M. Carrat and D.S. Soong, Macromolecules,
16, 348 (1983).
14. Y.B. Zeldovich and Y.A. Zysin, J. Technical Physics,
11, 502 (1941).
15. T. Furusawa and H. Nishimura, J. Chem. Eng. Japan,
1, 180 (1968).
16. V. Hlavacek, M. Kubicek and J. Jelinek, Chem. Eng. Sci.,
25, 1441 (1970).
17. A. Uppal, W.H. Ray and A. Poore, Chem. Eng. Sci., 31,
205 (1976).
18. D.T.J. Huang and A. Varma, Chem. Eng. Sci., 35, 1806
(1980).
19. M. Gohibitsky and B.L. Keyfitz, SIAM J. Math. Anal.,
11, 316 (1980).
20. V. Balakotaiah and D. Luss, Chem. Eng. Commun., 13,
111 (1981).
21. V. Balakotaiah and D. Luss, Chem. Eng. Sci., 37, 1611
(1982).
22. V. Balakotaiah and D. Luss, Chem. Eng. Sci., 37, 433
(1982).

23. V. Balakotaiah and D. Luss, Chem. Eng. Sci., 38, 1709 (1983).
24. V. Balakotaiah and D. Luss, A.I.Ch.E.J., 28, 552 (1983).
25. V. Balakotaiah and D. Luss, Chem. Eng. Sci., 39, 865 (1984).
26. R.S. Knorr and K.F. O'Driscoll, J. Appl. Polym. Sci., 14, 2683 (1979).
27. H. Gerrens, K. Kuchner and G. Ley, Chem. Eng. Technol., 43, 693 (1971).
28. R. Jaisinghani and W.H. Ray, Chem. Eng. Sci., 32, 811 (1977).
29. M. Nomura and M. Harada, ACS Symp. Ser., 165, 121 (1981).
30. J.W. Hamer, T.A. Akramov and W.H. Ray, Chem. Eng. Sci., 36(12), 1897 (1981).
31. A.D. Schmidt and W.H. Ray, Chem. Eng. Sci., 36, 1401 (1981).
32. B.W. Brooks, Chem. Eng. Sci., 36, 589 (1981).
33. K.Y. Choi and W.H. Ray, Chem. Eng. Sci., 40(12), 2261 (1985).
34. A.D. Schmidt, A.B. Clinch, and W.H. Ray, Chem. Eng. Sci., 39(3), 419 (1984).

35. K.Y. Choi, Polym. Eng. Sci., 26(14), 975 (1986).
36. P.E. Baillagou and D.S. Soong, Chem. Eng. Sci.,
40, 75 (1985).
37. B.M. Louie, G.M. Carrat and D.S. Soong, J. Appl.
Polym. Sci., 30, 3985 (1985).
38. P.E. Baillagou and D.S. Soong, Chem. Eng. Sci.,
40, 87 (1985).
39. B.M. Louie and D.S. Soong, J. Appl. Polym. Sci.,
30, 3707 (1985).
40. B. Kapoor, A. Varma and S.K. Gupta in preparation.
41. G.M. Carrat, C.R. Shervin and D.S. Soong, Polym.
Eng. Sci., 24, 442 (1984).

PMMA POLYMERIZATION IN CSIR : SIMULATION

DEFINITION OF VARIABLES

A, B = PARAMETER OF THE FOIJITA - DOLITTLE CORRELATION FOR (0/100).
 ALPHA = HEAT TRANSFER PARAMETER
 BETA = HEAT GENERATION PARAMETER
 DELTA = DIMENSIONLESS COOLANT TEMPERATURE
 0/100 = 0/100
 0/100 = RATIO OF DIFFUSIVITIES WITH GEL EFFECT TO THAT WITH GEL EFFECT
 EFF = INITIATOR EFFICIENCY
 EP = ACTIVATION ENERGY FOR PROPAGATION / R
 ET = ACTIVATION ENERGY FOR INITIATOR DECOMPOSITION / R
 ES = ACTIVATION ENERGY FOR TERMINATION / R
 FS = SOLVENT VOLUME FRACTION IN THE FEED
 INDEX2 = PARAMETER INDICATING CHOI'S RATE CONSTANT FOR INDEX2 = 1 AND SOONG'S RATE CONSTANT FOR INDEX2 = 2
 IQ = INITIATOR CONCENTRATION, GM - MOL/LIT
 INDEX1 = PARAMETER INDICATING GEL EFFECT FOR INDEX1 = 1 AND ABSENCE OF GEL EFFECT FOR INDEX1 = 2
 KO = INITIATOR DECOMPOSITION RATE CONSTANT
 KOO = PRE - EXPONENTIAL PART OF KO
 KT = TERMINATION RATE CONSTANT
 KTO = TERMINATION RATE CONSTANT IN ABSENCE OF GEL EFFECT
 KTOO = PRE - EXPONENTIAL PART OF KTO
 KP = PROPAGATION RATE CONSTANT
 KPO = PROPAGATION RATE CONSTANT IN ABSENCE OF GEL EFFECT
 KPOO = PRE - EXPONENTIAL PART OF KPO
 LDO = LIVE RADICAL POPULATION
 LDOKP = PRODUCT OF LDO AND KP
 T = TEMPERATURE IN DEG. K.
 TF = FEED TEMPERATURE
 DA = DAMKOLDER NUMBER
 PHIM = MONOMER VOLUME FRACTION
 RDM = DENSITY OF THE MONOMER AT THE REACTOR TEMPERATURE
 RDMO = DENSITY OF THE MONOMER AT THE FEED TEMPERATURE
 RPSS = VOLUME CONTRACTION PARAMETER, (RDP - RDM)/RDP
 RDMO / RDM
 DR = DENSITY RATIO, RDM/RDMO
 X1 = MONOMER CONVERSION
 X3 = DIMENSIONLESS TEMPERATURE

DIMENSION X(20)

INTEGER ITMAX, IER, N, NSIG, INDEX1, INDEX2, INT

COMMON ALPHA, BETA, TAU, INDEX1, INDEX2, FS, TF

EXTERNAL FUN

OPEN(UNIT=22, DEVICE='DSK', FILE='SIMS.OUT')

OPEN(UNIT=6, DEVICE='DSK')

=====

WRITE(5, 100)

READ(5, *) INDEX1

WRITE(5, 101)

READ(5, *) INDEX2

INDEX1 = 2 ; INDEX2 = 2

OPERATING CONDITIONS

FS = 0.6

TF = 300.0 ; EMEM = 100.0 ; DELHR = 13.5 ; RDCP = 0.4

```

ALPHA= 5000.0
RJM0 = 0.973 - 0.001164 * (TF -1 273.0)
EMEF = (1.0 -FS) * RJM0 * 1000.0/EMEM
BETA = DELHR * EMEF/(RDCP * TF) ; TYPE *,BETA

```

```

WRITE(22,700) ALPHA,BETA
FORMAT(5X,'ALPHA = ',F10.6,3X,'BETA=',E13.6/)
=====

```

```

N=6
TAU=0
IF(INDEX1.EQ.1) INT=100
IF(INDEX1.EQ.2) INT = 150
DO 102 M=1,INT
TYPE 556

```

```

FORMAT(5X,'I AM HERE')

```

```

X(1)=0.957
X(2)=0.85
X(3)=0.613
X(4)=0.291
X(5)=0.1
X(6) = 0.05

```

```

IF(INDEX1.EQ.1) PINC=30
IF(INDEX1.EQ.2) PINC = 1
TAU=TAU+PINC

```

```

IF(INDEX1.EQ.1) TIME=TAU/50
IF(INDEX1.EQ.1) TYPE 580,TIME
IF(INDEX1.EQ.2) TIME=TAU

```

```

IF(INDEX1.EQ.2) TYPE 581, TIME
FORMAT(5X,'TIME IN MINUTES = ',E13.6)
FORMAT(5X,'TIME IN HOURS=',E13.6/)
=====

```

```

EPS=1.0E-7 ; EPS2=1.0E-5 ; ETA=0.000001 ; NSIG=6 ; ITMAX=30
=====

```

```

CALL ZREAL1(FUN,EPS,EPS2,ETA,NSIG,N,X,ITMAX,IER)
CALL UERTST(IER,FUN)

```

```

IF(INDEX1.EQ.1) WRITE(22,1501) TIME
IF(INDEX1.EQ.2) WRITE(22,1502) TIME

```

```

FORMAT(/5X,'** TIME IN HOURS=',E13.6/)
FORMAT(5X,'** TIME IN MINUTES= ',E13.6/)

```

```

DO 555 J=1,5
IF(X(J).GT.1.0) GOTO 555
IF(X(J).LT.0.0) GOTO 555

```

```

X1 = X(J)
TYPE 181, X1
WRITE(22,181) X1
FORMAT(5X,'SOLUTION = ',E13.6)

```

```

CONTINUE
WRITE(22)

```

```

CONTINUE
FORMAT(5X,'TYPE IN THE VALUE OF INDEX1'/)
FORMAT(5X,'TYPE IN THE VALUE OF INDEX2'/)

```

```

STOP
END
=====

```

```

FUNCTION FUN(X1)
INTEGER INDEX1,INDEX2
REAL IO,KTO,KPO,KD,KP,KF,KPKPO,KTKTO,LDO KP,LDO
REAL TAU,EFF,EPSS,KF,KDO,KPO,KTO
COMMON ALPHA,BETA,TAU,INDEX1,INDEX2,FS,TF
EFF=0.58
IO=0.0258

```

```

IF(INDEX2.EQ.1) GOTO 1190
ED=15430.0 ; EP=2190.74 ; ET=352.733
K00=6.32E16 ; KP00=2.95E7 ; KT00=5.88E9
GOTO 1200
1190 ED=29600/1.987 ; EP=5300/1.987 ; ET=2800/1.987
1200 K00=5.95E13*60 ; KP00=7.0E6*50 ; KT00=3.52E9*60
CONTINUE
E=EP+0.5*(ED-ET)
KF=KP00*EXP(-E/TF)*SQRT(2.0*EFF*IO*K00/KT00)
TYPE*,KF
DELTA=0.01
DA=TAU*KF
X3=(BETA*X1+ALPHA*DA*DELTA)/(1.+ALPHA*DA)
T=TF*(1.0+X3)-273
KT0=KT00*EXP(-ET/(TF*(1.+X3)))
KP0=KP00*EXP(-EP/(TF*(1.+X3)))
KD=K00*EXP(-ED/(TF*(1.+X3)))
RJM0=0.973-0.001154*(TF-273.0)
EPSS=0.1945833+0.316565E-3*(TF*(1.+X3)-273.)
RJM=0.973-0.001154*(TF*(1.+X3)-273.0)
DR=RJM/RJM0
BS = 1.0
BS = FS/(1.0 - FS)
S = ((1.0 - EPSS * X1)/DR + BS)/(1.0 + BS)

A=0.168-8.17E-06*(TF*(1.+X3)-B37.0)**2
B=0.03
THETAT=3.372E-22/IO*EXP(17200.0/(TF*(1.0+X3)))
THETAP=5.48E-16*EXP(14000.0/(TF*(1.0+X3)))

LDOKP=S * X1/(1.0 - X1)/TAU
PHIM=(1.-X1)/(1.-EPSS*X1 + BS)
C=EXP(2.3*PHIM/(A+B*PHIM))
KPKP0=1.-THETAP*LDOKP/C
KP=KPKP0*KP0
LD0=LDOKP/KP
KTKT0=1./(1.+THETAT*KT0*LD0/ED)
KT=KTKT0*KT0
TYPE 481,KTKT0,KPKP0
FORMAT(5X,'KTKT0=',E13.6,5X,'KPKP0=',E13.6)
-----
EVALUATION OF THE FUNCTION F
-----
IF(INDEX1.EQ.2)GOTO 115
KT=KT0 ; KP=KP0
CONTINUE
FUNC1=2.0*EFF*IO*(KP**2)*KD/KT*(TAU**2)
IF(INDEX1.EQ.4) S = 1.0
F2=( S * X1/(1.0 - X1))**2
R =KD*TAU + S
FUNC2=F2 * R
FUN=(FUNC1)-1*(FUNC2)
TYPE*, X1, FUN
RETURN
END

```

```

FVEC(2) = 2.0 * EFF * ID * FAJ **2 * ( KP **2/KT * DKDDX1 - KP
1      **2/KT **2 * KD * DKTDX1 + 2.0 * KP * KD/KT * DKPDX1 )
2      -( DF2DX1 * R + DRDX1 * F2 )
FVEC31 = KP **2 * D2KD/KT - (KP/KT) **2 * DKDDX1 * DKTDX1 + 2.0 *
1      KP/KT * DKPDX1 * DKDDX1
FVEC32 = KP **2 * KD/KT **2 * D2KT + (KP/KT) **2 * DKDDX1 * DKTD
1      X1 + 2.0 * KP * KD/KT **2 * DKPDX1 * DKTDX1 - 2.0 * KP
2      **2 * KD * DKTDX1 ** 2 /KT **3
FVEC33 = KP * KD/KT * D2KP + KP/KT * DKDDX1 * DKPDX1 + KD/KT *
1      DKPDX1 **2 - KP * KD/KT **2 * DKPDX1 * DKTDX1
FVEC(3) = 2.0 * EFF * ID * FAJ **2 * (FVEC31 - FVEC32 + 2.0 *
1      FVEC33) - FVEC34
* -----
TYPE 2 , X1 , ALPHA1 , DA
ALPHA1 = ALPHA * KF ; FAJ1 = FAJ/50.0
22 TYPE 22 , ALPHA1 , FAJ1
FORMAT( ' ALPHA1 = 'E13.6,3X, 'FAJ1 = 'E13.6/)
TYPE 3 , FVEC(1) , FVEC(2) , FVEC(3)
2
3 FORMAT( 2X, 'X1= 'F10.7,3X, 'ALPHA = 'F13.6,3X, 'DA = 'F10.6/)
FORMAT(5X, 'FVEC(1) = 'E13.6 ,3X, 'FVEC(2)= 'E13.6,3X, 'FVEC(3)=
1      'E13.6/)
* -----
RETURN
END

```

```

DC2DX1 = 2.0 * (A + B * PHIM) * (DADX1 + B * DPHIM)
D2CDX1 = 2.3 * (C2 * DC1DX1 - C1 * DC2DX1) / C2 **2

DT11 = -THETAP * KP0/C **2 * D2CDX1 - DCDX1 * THETAP * DKP0DX/C
1      **2 - DCDX1 * KP0/C **2 * DTHER + 2.0 * THETAP * KP0/C
2      **3 * DCDX1 **2
DT12 = THETAP/C * D2KP0 + DKP0DX/C * DTHER - THETAP/C **2 *
1      DCDX1 * DKP0DX
DT13 = KP0/C * DTHER2 + DKP0DX/C * DTHER - KP0/C **2 * DTHER *
1      DCDX1

DT1DX1 = DT11 + DT12 + DT13

DL0KP2 = ( X1 * D2S / (1.0 - X1) + 2.0 * DSDX1 / (1.0 - X1) **2 + 2.0
1      * S / (1.0 - X1) **3 ) / PAU

D2KP = D2KP0 - L00KP * DT1DX1 - 2.0 * T1 * DL0KP - THETAP * KP0
1      /C * DL0KP2

DL0D2 = DL0KP2/KP - 2.0 * DL0KP * DKPDX1/KP **2 - L00KP * D2KP
1      /KP **2 + 2.0 * L00KP/KP **3 * DKPDX1 **2

DP1 = THETAT * LD0 * KT0/C * (D2CDX1/C - (DCDX1/C) **4) + DCDX1 *
1      DPDX1/C

DP2 = THETAT * LD0/C * D2KT0 - THETAT * LD0/C **2 * DKT0DX * DC
1      DX1 + THETAT/C * DL00 * DKT0DX + LD0/C * DTHER * DKT0DX

DP3 = THETAT * KT0/C * DL0D2 - THETAT * KT0/C **2 * DPDX1 * DL00
1      + THETAT/C * DKT0DX * DL00 + KT0/C * DTHER * DL00

DP4 = LD0 * KT0/C * DTHER2 - LD0 * KT0/C **2 * DCDX1 * DTHER +
1      LD0/C * DKT0DX * DTHER + KT0/C * DL00 * DTHER

D2PDX1 = -DP1 + DP2 + DP3 + DP4

D2KT = (P * D2KT0 - KT0 * D2PDX1) / P **2 - 2.0 / P **3 * (P * DKT0DX
1      - KT0 * DPDX1) * DPDX1
TYPE 19, DPDX1
FORMAT(' ', DPDX1 = 'E13.6/')

-----
CALCULATION OF THE FUNCTION VALUES
-----
CONTINUE

F1 = KP **2 * KD/KT ; F2 = (S * X1 / (1.0 - X1)) **2
R = S + KD * PAU
DRDX1 = DSDX1 + PAU * DKDDX1
DF2DX1 = 2.0 * S * X1 / (1.0 - X1) **2 * ( X1 * DSDX1 + S / (1.0 - X1) )

D2R = D2S + PAU * D2KD
D2F2 = 2.0 * S * X1 / (1.0 - X1) **2 * (DSDX1 + X1 * D2S + 1 / (1.0
1      - X1) **2 * (DSDX1 * (1.0 - X1 + S)) + 2.0 * (DSDX1 * X1
2      + S / (1.0 - X1)) * (DSDX1 * X1 / (1.0 - X1) **2 + S * (1.
3      + X1) / (1.0 - X1) **3)

FVEC34 = D2F2 * R + 2.0 * DF2DX1 * DRDX1 + D2R * F2
FVEC(1) = 2.0 * EFF * I0 * PAU **2 * F1 - F2 * R

```

19

*
C
*
10

```

1      (1.0 + X3 ) ** 2 )
DTHET = -17200.0 * BETA * THETAP / ( TF * (1.0 + ALPHA * DA) *
1      ( 1.0 + X3 ) ** 2 )
DADX1 = -16.34 E-5 * IF * BETA/(1.0 + ALPHA * DA) * (T - 337)
DF3DX1 = 0.001164 * IF * RDM * BETA/(1.0 + ALPHA * DA)/RDM**2
DEPSX = EPSS + 0.916E-3 * BETA * IF * X1/(1.0 + ALPHA * DA)
DSDX1 = ((1.0 - EPSS * X1) * DF3DX1 - F3 * DEPSX)/(1.0 + BS)
DPHIM = ((1.0 - X1) * DEPSX - (1.0 + EPSS * X1 - BS)/
1      (1.0 - EPSS * X1 + BS)**2)
DCDX1 = 2.3 * C * ( A * DPHIM - PHIM * DADX1)/(A + B * PHIM) **2
DL0KP = ( S/(1.0 - X1)**2 + DSDX1 * X1/(1.0 - X1))/TAU
DKPODX1 = DKPODX - L0KP * (-DCDX1 * THETAP * KP0/C **2 +
1      (THETAP * DKPODX + KP0 * DIHEP)/C) - THETAP * KP0/C *
2      DL0KP
DL00 = (DSDX1 * X1/(KP * (1.0 - X1)) - S * X1 * DKPODX1/
1      (KP **2 * (1.0 - X1)) + S/(KP * (1.0 - X1)**2))
2      /TAU
DPDX1 = -THETAP * L00 * KP0 * DCDX1/C **2 + THETAP * L00/C *
1      DKPODX + THETAP * KP0 * DL00/C + L00 * KP0/C * DIHEP
DKTDX1 = ( P * DKPODX - KT0 * DPDX1 )/P **2
-----
CALCULATION OF THE SECOND DERIVATIVES
-----
DENOM = IF * (1.0 + ALPHA * DA) * (1.0 + X3 ) **3
DIHEP2 = - 14000.0 * BETA /DENOM * (DIHEP * (1.0 + X3) - 2.0 *
1      THETAP * BETA/(1.0 + ALPHA * DA))
DTHET2 = -17200.0 * BETA /DENOM * (DTHET * (1.0 + X3 ) - 2.0 *
1      THETAP * BETA/ ( 1.0 +ALPHA * DA))
FI = -THETAP * KP0 * DCDX1/C **2 + (THETAP * DKPODX + KP0 *
1      DIHEP)/C
D2ADX1 = -16.34 E-5 * (IF * BETA/(1.0 +ALPHA * DA)) **2
D2F3 = 2.0 * DF3DX1 ** 2/F3
DEPSX2 = 1.832E-3 * IF * BETA/(1.0 + ALPHA * DA)
D2S = (D2F3 * (1.0 - EPSS * X1) - 2.0 * DF3DX1 * DEPSX - F3 *
1      DEPSX2) /(1.0 +BS)
R1 = (1.0 - X1) * DEPSX - (1 + EPSS * X1 - BS
R2 = (1.0 - EPSS * X1 + BS) **2
DR1DX1 = (1.0 - X1) * DEPSX2
DR2DX1 = 2.0 * (1.0 - EPSS * X1 + BS) * (- DEPSX)
DPHIM2 = ( R2 * DR1DX1 - R1 * DR2DX1)/R2 **2
C1 = C * (A * DPHIM - PHIM * DADX1) ; C2 = (A + B * PHIM)**2
DC1DX1 = C * (A * DPHIM2 - PHIM * D2ADX1) + DCDX1 * C1/C

```



```
TYPE * ,KF
```

```
-----
FIRST DERIVATIVES OF RATE CONSTANTS W. R. TO X1
-----
```

```
DTDX1 = IF * BETA / (1.0 + ALPHA * DA)
```

```
DBT = - DTDX1 / T **2
```

```
DKTODX = -KT0 * ET * DBT
```

```
DKPODX = -KP0 * EP * DBT
```

```
DKDDX1 = -KD * ED * DBT
```

```
-----
SECOND DERIVATIVES OF THE RATE CONSTANTS
-----
```

```
DBT2 = 2.0 * (DTDX1) **2 / T **3
```

```
D2KT0 = -ET * (DKPODX * DBT + KT0 * DBT2)
```

```
D2KP0 = -EP * (DKPODX * DBT + KP0 * DBT2)
```

```
D2KD = -ED * (DKDDX1 * DBT + KD * DBT2)
```

```
-----
SWITCH OVER TO NO GEL EFFECT CASE
-----
```

```
IF (NGEL .EQ. 2) GOTO 8
```

```
KP = KP0 ; KT = KT0 ; DKPODX1 = DKPODX ; DKTDX1 = DKTDX
```

```
D2KP = D2KP0 ; D2KT = D2KT0 ; D2KD = D2KD
```

```
S = 1.0 ; DSDX1 = 0.0 ; D2S = 0.0
```

```
GOTO 10
```

```
-----
CALCULATION OF THE PHYSICAL PROPERTIES FOR GEL EFFECT CASE
-----
```

```
CONTINUE
```

```
RDM0 = 0.973 - 0.001164 * (TF - 273.0)
```

```
EPSS = 0.1945833 + 0.91656E-3 * (TF - 273.0)
```

```
RDM = 0.973 - 0.001164 * (TF - 273.0)
```

```
F3 = RDM0/RDM
```

```
DR = RDM/RDM0
```

```
BS = FS / (1.0 - FS)
```

```
S = (BS + (1.0 - EPSS * X1) / DR) / (1.0 + BS) ! FS = SOLVENT VOLUME FRACTION
```

```
LOOKP = S * X1 / (1.0 - X1) / TAU ! FROM MONOMER BALANCE
```

```
TYPE * , LOOKP
```

```
THETAP = 5.48 E-15 * EXP (14000.0/T)
```

```
THETAT = 3.372 E-22 / T * EXP (17200.0/T)
```

```
A = 0.168 - 8.47E-06 * (T - 387.0) **2
```

```
B = 0.03
```

```
PHIM = (1.0 - X1) / (1.0 - EPSS * X1 + BS)
```

```
CP02 = EXP (2.3 * PHIM / (A + B * PHIM))
```

```
KP02 = THETAP * LOOKP / C * KP0
```

```
KP = KP0 - THETAP * KP0 * LOOKP / C
```

```
GP = KP / KP0
```

```
L00 = LOOKP / KP
```

```
TYPE * , THETAP, KP0, LOOKP, C
```

```
P = 1.0 + THETAT * L00 * KT0 / C
```

```
KT = KT0 / P
```

```
GT = KT / KT0
```

```
TYPE 32, GP, GT
```

```
FORMAT (' GP = 'E13.6, 3X, ' GT = 'E13.6/)
```

```
-----
CALCULATION OF THE FIRST DERIVATIVE OF THE RATE CONSTANTS
-----
```

```
DTHEP = -14000.0 * BETA * THETAP / (TF * (1.0 + ALPHA * DA) *
```

```
*
C
*
```

```
*
L
*
```

```
*
C
*
```

```
*
L
3
```

```
*
```

```
32
```

```
*
C
*
```

```

WRITE(22,4) FS, BETA
WRITE(22,1) FNORM, IFAIL, (X(J), J=1,3)
FORMAT(2X, 'FNORM='E13.6/2X, 'IFAIL='I3/2X, 'X(1)='X(1)/2X, 'X(2)='X(2)/2X, 'X(3)='X(3)/2X, 'BETA='E13.6)
FORMAT(2X, '** FS ='F10.6/5X, '** BETA ='F10.7/)
FORMAT(5X, 'TYPE IN THE VALUE OF NGEL' /5X, 'NGEL=1 MEANS NO GEL EFFECT' /5X, 'NGEL=2 MEANS GEL EFFECT' /)
TYPE *X(1), X(2), X(3), FNORM
FORMAT(5X, 'TYPE IN THE VALUE OF BETA' /)
FORMAT(5X, 'TYPE IN THE INITIAL GUESSES' /5X, 'X(1), X(2), X(3)=' /)
FORMAT(5X, 'TYPE IN THE VALUE OF INDEX' /5X, 'INDEX=1 MEANS CHOI'
IS RATE CONSTANTS' /5X, 'INDEX=2 MEANS SOONG'S RATE CONST.' /)
IF(BETA.GT.1.0) STOP
GOTO 801
STOP
END

```

----- SUBROUTINE FOR THE EVALUATION OF THE FUNCTIONS -----

```

SUBROUTINE FCN (N, X, FVEC, IFLAG)
REAL X(N), FVEC(N)
INTEGER NGEL, INDEX, IFLAG, N
REAL IO, KF, KP, KPKPO, KP, KTKTO, KP00, KT00, KDO, KO, LOOKP, LOO,
1 IF, EFF, EPSS, ROM, ROAD, A, B, C, THETAP, THETAP
COMMON BETA, NGEL, INDEX, FS, TF

```

----- OPERATING CONDITIONS -----

```

IO = 0.0258 ; EFF = 0.58 ; DELTA = 0.01

```

```

X1 = X(1) ; ALPHA = X(2) ; DA = X(3)
X3 = (BETA * X1 + ALPHA * DA * DELTA) / (1.0 + ALPHA * DA)
I = TF * (1.0 + X3)
IF (INDEX.EQ.1) GOTO 11
IF (INDEX.EQ.2) GOTO 5

```

----- CHOI'S RATE CONSTANTS -----

```

11 KP00 = 4.2E08 ; KT00 = 2.112E11 ; KDO = 3.57 E13
EP = 3170.609 ; ET = 1409.0595 ; ED = 14896.829
GOTO 6

```

----- SOONG'S RATE CONSTANTS -----

```

5 KP00 = 2.95E07 ; KT00 = 5.33E09 ; KDO = 6.32E18
EP = 2189.23 ; ET = 352.793 ; ED = 15430.3

```

----- RATE EXPRESSIONS -----

```

6 KP0 = KP00 * EXP(-EP/I)
KT0 = KT00 * EXP(-ET/I)
KD = KDO * EXP(-ED/I)

```

----- DEFINITION OF DAMKOHLEH NUMBER -----

```

E = EP + 0.5 * (ED - ET)
KF = KP00 * EXP(-E/TF) * SQRT(2.0 * EFF * IO * KDO/KT00)
TAU = DA/KF

```


HYSTERESIS VARIETY FOR P4MA

DEFINITION OF VARIABLES

A, B = PARAMETER OF THE FOJITA - DOLITTLE CORRELATION FOR (D/DO).
 ALPHA = HEAT TRANSFER PARAMETER
 BETA = HEAT GENERATION PARAMETER
 DELTA = DIMENSIONLESS COOLANT TEMPERATURE
 D/DO = RATIO OF DIFFUSIVITIES WITH GEL EFFECT TO THAT WITH GEL EFFECT.
 EFF = INITIATOR EFFICIENCY
 EP = ACTIVATION ENERGY FOR PROPAGATION / R
 ED = ACTIVATION ENERGY FOR INITIATOR DECOMPO. / R
 ET = ACTIVATION ENERGY FOR TERMINATION / R
 FS = SOLVENT VOLUME FRACTION IN THE FEED
 INDEX = PARAMETER INDICATING CHOI'S RATE CONSTANT FOR INDEX = 1 AND SOONG'S RATE CONSTANT FOR INDEX = 2
 IO = INITIATOR CONCENTRATION, GM - MOL/LIT
 NGEL = PARAMETER INDICATING GEL EFFECT FOR NGEL = 1 AND ABSENCE OF GEL EFFECT FOR NGEL = 2
 KO = INITIATOR DECOMPOSITION RATE CONSTANT
 KDO = PRE - EXPONENTIAL PART OF KO
 KI = TERMINATION RATE CONSTANT
 KTO = TERMINATION RATE CONSTANT IN ABSENCE OF GEL EFFECT
 KTOC = PRE - EXPONENTIAL PART OF KTO
 KP = PROPAGATION RATE CONSTANT
 KPO = PROPAGATION RATE CONSTANT IN ABSENCE OF GEL EFFECT
 KPOC = PRE - EXPONENTIAL PART OF KPO
 LDO = LIVE RADICAL POPULATION
 LOOKP = PRODUCT OF LDO AND KP
 T = TEMPERATURE IN DEG. K.
 TF = FEED TEMPERATURE
 DA = DAMKOLHER NUMBER
 PHIM = MONOMER VOLUME FRACTION
 RDM = DENSITY OF THE MONOMER AT THE REACTOR TEMPERATURE
 RDMO = DENSITY OF THE MONOMER AT THE FEED TEMPERATURE
 EPSS = VOLUME CONTRACTION PARAMETER, (RDP - RDM)/RDP
 F3 = RDMO / RDM
 DR = DENSITY RATIO, RDM/RDMO
 TAU = MEAN RESIDENCE TIME IN MIN.
 THETAP, THETAT = PARAMETERS IN THE GLASS AND GEL EFFECT MODEL OF CHIU ET AL. RESPECTIVELY
 X1 = MONOMER CONVERSION
 X3 = DIMENSIONLESS TEMPERATURE
 DCDX1 = FIRST DERIVATIVE OF C1 WITH RESPECT TO X1
 DADX1 = FIRST DERIVATIVE OF A W.R. TO X1
 D2ADX1 = SECOND DERIVATIVE OF A W.R. TO X1
 D2CDX1 = SECOND DERIVATIVE OF C1 W.R. TO X1
 DTDX1 = FIRST DERIVATIVE OF TEMPERATURE W.R. TO X1
 DBT = FIRST DERIVATIVE OF (1/T) W.R. TO X1
 DBT2 = SECOND DERIVATIVE OF (1/T) W.R. TO X1
 D = FIRST DERIVATIVE OF LDO W.R. TO X1
 DLDKP = FIRST DERIVATIVE OF LOOKP W.R. TO X1
 DLDU2 = SECOND DERIVATIVE OF LDO W.R. TO X1
 DLDKP2 = SECOND DERIVATIVE OF LOOKP W.R. TO X1
 DKTDX1 = FIRST DERIVATIVE OF KI W.R. TO X1
 DKTODX = FIRST DERIVATIVE OF KTO W.R. TO X1
 DKPDX1 = FIRST DERIVATIVE OF KP W.R. TO X1
 DKPODX = FIRST DERIVATIVE OF KPO W.R. TO X1
 DKDODX1 = FIRST DERIVATIVE OF KO W.R. TO X1

2. BATCH REACTOR SIMULATION : RUNGE-KUTTA

```

DIMENSION YPRIME(10) , Y(10)
INTEGER RUNGE
REAL KP , KT , KD , KPO , KTO , IO , LDO , LDOO , L ,
1 KPKPO , KTKTO
OPEN (UNIT = 22 , DEVICE = 'DISK' , FILE = 'BATCH.DAT')

```

```

H = 0.001
IREQ = 1000
X = 0.0
XEND = 30.0
ICOUNT = 1
TF = 300.0
T = 363.0
IO = 0.01548

```

3. INITIAL CONDITIONS

```

Y(1) = 0.0
Y(2) = IO
Y(3) = 0.0

```

```

WRITE(22, 100)
WRITE(22, 200) T , IO
WRITE(22, 300)

```

```

111 K = RUNGE(3 , Y , YPRIME , X , H)
IF( K .EQ. 1) GO TO 113
X1 = Y(1) ; I = Y(2) ; LDO = Y(3)

KPO = 5.88 E9 * EXP( - 352.793/T )
KPO = 2.95 E7 * EXP( - 2190.74/T )
KD = 6.32 E16 * EXP( - 15430.0/T )

EPSS = 0.1945833 + 0.916567 E-31 * (T - 273.0)
EPSS = - EPSS
A = 0.168 - 8.17 E-06 * (T - 1337.0) ** 2
B = 0.03
THETAP = 5.4814 E-16 * EXP( 13932.0/T )
THETAT = 1.1353 E-22/IO * EXP( 17420.0 /T )

PHIM = (1.0 - X1)/(1.0 + EPSS * X1)
C = EXP( 2.303 * PHIM/(A + B * PHIM))

KPKPO = 1.0/(1.0 + THETAP * KPO * LDO/C)
KTKTO = 1.0/(1.0 + THETAT * KTO * LDO/C)

KP = KPKPO * KPO
KT = KTKTO * KTO

EFF = 0.58
YPRIME(1) = KP * (1.0 - X1) * LDO
YPRIME(2) = -KD * I - KP * (1.0 - X1) * LDO * EPSS * I /
1 (1.0 + EPSS * X1)

```

```
YPRIME (3) = 2.0 * EFF * KD * I - I * KP * (LDO ** 2) - KP * (1.0  
1 - X1) * EPSS * (LDO ** 2) / (1.0 + EPSS * X1)
```

```
GOTO 111
```

```
113 IF(X. LE. XEND) GOTO 116  
STOP
```

```
115 ICDUNT = ICDUNT + 1  
IF(ICDUNT. LT. IREQ) GOTO 141  
TYPE * X , X1 , I , LDO  
WRITE(22 , 4000 'X' , X1  
ICDUNT = 1  
GOTO 111
```

```
100 FORMAT( 10X, 'BATCH REACTOR SIMULATION'//)  
200 FORMAT( 10X, 'TEMPERATURE = 'F10.6' DEG. K. ' /10X, 'INITIATOR  
1 LOADING = 'F10.6' MOL/L ' //)
```

```
300 FORMAT(10X, ' TIME IN MIN. ' , 5X, 'MONOMER CONV. ' //)
```

```
400 FORMAT(20X,F10.6,10X,E13.6)
```

```
END
```

```
C SUBROUTINE RUNGE -I KUTTA
```

```
FUNCTION RUNGE ( N , Y , F , X , H)  
INTEGER RUNGE  
DIMENSION PHI(50) , SAVEY(50) , Y(N) , F(N)  
DATA M/0/  
M = M + 1  
GOTO (1 , 2 , 3 , 4 , 5) , M
```

```
1 RUNGE = 1  
RETURN  
2 DO 22 J = 1 , N  
SAVEY ( J ) = Y ( J)  
PHI(J) = F(J)  
22 Y(J) = SAVEY(J) + 0.5 * H * F(J)  
X = X + 0.5 * H  
RUNGE = 1  
RETURN
```

```
3 DO 33 J = 1 , N  
PHI( J ) = PHI( J ) + 2.0 * F ( J)
```

```
33 Y(J) = SAVEY(J) + 0.5 * H * F ( J)  
RUNGE = 1  
RETURN
```

```
4 DO 44 J = 1 , N  
PHI(J) = PHI(J) + 2.0 * F ( J)  
44 Y(J) = SAVEY( J ) + H * F(J)  
X = X + 0.5 * H  
RUNGE = 1
```

```
5 DO 55 J = 1 , N  
55 Y(J) = SAVEY(J) + ( PHI(J) + F(J)) * H/6  
M = 0
```

```
RUNGE = 0  
RETURN  
END
```